Universiteit Utrecht

Department of Mathematics

Master's Thesis

Measuring wake turbulence using Mode S radar data

Daily supervisor:
M.R. Opbroek (LVNL)

Author:
C.C.E. Smans

Project supervisor:
R.H. Bisseling (UU)

Second reader:
P.A. Zegeling (UU)

Universiteit Utrecht

July 1, 2021

Acknowledgements

This research was part of an internship at Air Traffic Control the Netherlands (LVNL). I would first like to thank my supervisor Marcel Opbroek from LVNL for his insights and support during the internship. In addition, I thank my supervisor Rob Bisseling from the Mathematics department at Utrecht University for the supporting conversations and helpful comments.

Abstract

Increasing landing capacity is important to reduce delays and therefore costs, fuel burn and emissions. Decreasing separation distances between aircraft is a way to increase the landing capacity. A safe distance between aircraft depends, among other things, on the level of turbulence an aircraft experiences. Turbulence can be caused by wind or weather conditions, but also by wake vortices generated by nearby aircraft. Therefore, aircraft cannot fly too close behind each other and separation minima have been established by ICAO. To increase landing capacity, LVNL will implement a recategorisation and time based separation, a project which is called RECAT-TBS, at Amsterdam Airport Schiphol by the end of this year to safely decrease these separation minima.

The goal of this thesis is to implement an algorithm that can detect and measure wake turbulence in the approach area using Mode S radar data. This can give insight in a possible increase in the number of wake turbulence encounters or might yield a warning system when decreasing the separation distances in final approach by the end of this year. The algorithm that will be analysed is an algorithm proposed in a paper by Xavier Olive and Junzi Sun [10]. They implemented and analysed the algorithm for en-route air traffic to detect turbulence. The question is whether this algorithm can also be used or adapted to be applicable for approaching air traffic and if it is possible to distinguish wake turbulence encounters.

Contents

Chapter 1

Introduction

Wake turbulence is an important factor for a safe separation between aircraft in the approach area of an airport. It is caused by wake vortices generated by nearby aircraft. Dangerous situations can occur when aircraft fly into the wake vortices of the aircraft in front. Therefore, the International Civil Aviation Organisation (ICAO) has determined separation minima for safe landings of all aircraft [16].

With a continuing growth in air traffic, increasing airport capacity becomes more important. Until the COVID-19 pandemic, the number of landings and take-offs at Amsterdam Airport Schiphol increased from 386.400 in 2010 to 496.800 in 2019 [11]. Air traffic will be back on this level by 2024 at the earliest and will increase further from there [3]. How to increase airport capacity, especially landing capacity, is a question that is studied for years now and is important for reducing delays and therefore also costs, fuel burn and emissions.

Landing capacity can be increased by decreasing separation distances between aircraft in their final approach. Since ICAO separation minima lead to over-separation in many situations, Air Traffic Control the Netherlands (LVNL) plans to implement a recategorisation and time based separation (RECAT-TBS) to safely decrease the separation minima. Aircraft flying closer behind each other might lead to an increase in wake turbulence experienced. Hence, being able to detect and measure the turbulence caused by wake vortices is useful to get insight in the number of wake turbulence encounters. Therefore, the main goal of this research is to see whether it is possible to detect and measure wake turbulence effects on aircraft during landing.

In a recent study [10], Xavier Olive and Junzi Sun propose a method to detect and measure turbulence experienced by en-route air traffic based on widely available radar data. The key parameters used for their method are two different sources for vertical speed: the barometric vertical rate and the inertial vertical velocity. Due to incomplete filtering, the barometric vertical rate contains significant noise which is filtered

out in the inertial vertical velocity [17]. The main idea of their proposed method is that turbulence causes a major part of the noise. Therefore, the difference between noise in the barometric measure and in the inertial measure is analysed and used as a measure for turbulence.

Where Olive and Sun tested the method on en-route air traffic and detected not only turbulence caused by wake vortices, in this thesis the proposed method will be analysed and adapted to be applicable for detecting specifically wake turbulence in approaching air traffic. The goal of this is to give insight in the number of wake vortex incidents and possibly yield a warning system for air traffic controllers.

In Chapter 2, we start with a little background literature which is helpful to understand the problem. Next, in Chapter 3, we will describe the method used in this thesis including a description of the data, the algorithm and validation of the algorithm. Conducted experiments to improve the algorithm, together with its results, are described in Chapter 4. Finally, we will draw our conclusions, discuss the research and propose future work in Chapter 5.

Chapter 2

Background literature

In this chapter, we will give a little background literature which is helpful to understand the problem. First, we explain what wake turbulence is and how the separation distances between aircraft are based on this. Second, we describe how the data used for this research is obtained from Mode S radars. At last, we will shortly describe the approach of an aircraft, since this research will mainly focus on approaching air traffic.

Figure 2.1: Illustration of wake vortices [15].

2.1 Wake turbulence and aircraft separation

As mentioned before, wake turbulence is caused by wake vortices generated by nearby aircraft. A wake vortex is defined as the turbulent airflow which follows an aircraft. It is formed behind the wingtips due to air moving from the high pressure area below the wing to the low pressure area on top of the wing. An illustration of wake vortices

is shown in Figure 2.1. Especially during takeoff and landing there is a big difference in pressure below and on top of the wing which causes strong wake vortices. The strength of the wake vortex is furthermore affected by the weight and speed of the aircraft and shape of the wing. The heavier the aircraft or the slower the speed, the stronger the wake vortices. If the separation distance between aircraft is too small such that the trailing aircraft ends up in the wake vortex of the leading aircraft, this can in worst case cause the aircraft to roll over and crash. Therefore, the strength of the wake vortex is an important factor in determining a minimum separation distance between aircraft [16].

Due to the difference in wake vortices among different types of aircraft, the minimum separation distance depends on both the type of the leading and the trailing aircraft. Till now, aircraft are grouped into four wake turbulence categories (WTC), defined by the International Civil Aviation Organisation (ICAO): super heavy, heavy, medium and light. The super heavy category includes only the A380, the largest passenger aircraft that exists that generates wake vortices much bigger than aircraft in the heavy category. The minimum separation distances, in nautical mile (NM), for all combinations of leading and trailing aircraft can be found in Table 2.1 [13]. The minimum radar separation (MRS) in the terminal manoeuvring area (TMA) is 3.0 NM [14].

Leader/Follower	Super	Heavy	Medium	Light
Super	MRS	6.0 NM	7.0 NM	8.0 NM
Heavy	MRS	4.0 NM	5.0 NM	6.0 NM
Medium	MRS	MRS	MRS	5.0 NM
Light	MRS	MRS	MRS	MRS

Table 2.1: Minimum separation distances under ICAO criteria.

Using the ICAO criteria might lead to over-separation. In the past few years, research on wake vortex behaviour by the European Organisation for the Safety of Air Navigation (EUROCONTROL) made it possible to improve the categorisation. They developed a re-categorisation of the ICAO wake turbulence categories, named RECAT-EU. Their research proved that not only weight but also speed and wingspan are important factors for the strength of the wake vortex and therefore also for the minimum separation distance. Due to this, aircraft are grouped into six new categories: super heavy (A), upper heavy (B), lower heavy (C), upper medium (D), lower medium (E) and light (F). For all new leader and follower combinations, new separation minima were defined. These are shown in Table 2.2 [13].

Leader/Follower	A	B	C	D	E	F
A	MRS	4.0 NM	5.0 NM	5.0 NM	6.0 NM	8.0 NM
B	MRS	MRS	4.0 NM	4.0 NM	5.0 NM	7.0 NM
C	MRS	MRS	MRS	MRS	4.0 NM	6.0 NM
D	MRS	MRS	MRS	MRS	MRS	5.0 NM
E	MRS	MRS	MRS	MRS	MRS	4.0 NM
F	MRS	MRS	MRS	MRS	MRS	MRS

Table 2.2: RECAT-EU minimum separation distances.

In March 2016, RECAT-EU was first implemented at the airport Paris Charles de Gaulle. It led to a maximum reduction of 30% of separation distances, depending on the types of aircraft landing in a period. The result is an extra 2-4 aircraft landing per hour during peak hours [7]. The Netherlands Aerospace Centre (NLR) researched the benefits for Amsterdam Airport Schiphol. They focused on peak times and concluded that during morning peak time, when many heavy aircraft land, it would increase the landings per hour by one. During afternoon peak time, when mostly medium aircraft land, this increase is less. The lower benefits at Amsterdam Airport Schiphol when compared to Paris Charles de Gaulle can be explained by the fact that there are more heavy aircraft landing in Paris [1].

On top of RECAT-EU, EUROCONTROL started researching Time Based Separation (TBS) to improve the minimum separation distances. Till now, the separation between aircraft is a distance based separation. TBS is a concept that bases the minimum separation between aircraft on time instead of distance. Since aircraft take longer time to fly a certain distance if there is strong headwind, less aircraft are landing per hour in this situation. Strong headwinds are a big cause of delays. However, although slowing down aircraft, stronger headwind does make wake turbulence dissipate more quickly. This means that a smaller separation distance between aircraft is safe if headwind is strong. Hence, if minimum separation is based on time, the same number of aircraft can land per hour, strong headwinds or not [5].

National Air Traffic Services of the UK (NATS) implemented TBS at London Heathrow Airport in March 2015. At London Heathrow Airport, strong winds caused 44% of all air traffic flow management delays. TBS reduced these delays already with 62% and made it possible to land, on average, 20 extra aircraft per day [8]. The goal is to have implemented TBS by 2023 at many more European airports, including Amsterdam Airport Schiphol [5]. Air Traffic Control The Netherlands (LVNL) plans to implement RECAT-EU together with TBS in 2021, called RECAT-TBS [1].

For a safe use of RECAT-TBS, it is useful to know whether wake turbulence experi-

enced by aircraft increases when flying closer behind each other. Aircraft are able to measure turbulence themselves, but this information is rarely available for air traffic controllers. Therefore, this research uses data that is widely available obtained from Mode S radars.

2.2 Mode S radars

In air traffic control, two types of radars are used: primary surveillance radars and secondary surveillance radars. A primary radar system measures the position of a target by using reflections of radio signals. The radar sends a pulse, the aircraft reflects this pulse and the radar detects this reflection. Using the time between sending the pulse and detecting the reflection, together with the position of the radar, the two-dimensional position of the aircraft can be determined. A secondary surveillance radar is a radar system that uses interrogators and transponders to obtain information from the aircraft. The ground-based interrogator sends pulses that include a request. These are received by the transponder aboard the aircraft. The transponder decodes the request, obtains the requested information and transmits a coded reply signal containing the requested information back to the radar.

Mode S is a secondary surveillance radar technique which is required for aircraft transponders and radars since 2008. It contributes to the safety of Dutch airspace since aircraft with Mode S transponders are visible for the Airborne Collision Avoidance System (ACAS) and at the radar display for air traffic controllers. Mode S is a selective radar system which means that it can send requests, using the same technique as conventional radars, to specific aircraft instead of to the whole airspace reachable for the radar. To be able to do this, all aircraft are assigned a unique 24-bit address, the ICAO address. Information requested by Mode S radars comes in aircraft Comm-B Data Selector (BDS) registers. A BDS code in the radar request determines which register with its content has to be transmitted. If a Mode S radar sends a request for a BDS register, the transponder transmits a coded message containing all parameters contained in this BDS register. The surveillance information is coded using the ASTERIX data format. ASTERIX, short for All purpose Structured Eurocontrol Surveillance Information Exchange, was developed for surveillance data transmission and has different categories, each category dealing with a different type of information [2]. ASTERIX coded messages are decoded in ARTAS, a EUROCONTROL system that processes surveillance data and distributes the processed information to many user systems used by air traffic controllers. ARTAS merges data obtained from many radars, each with its own update rate. The processed information contains data with an update for every four seconds, which means that every four seconds the latest obtained radar information is added.

Mode S contains two most used services, Elementary Surveillance (ELS) and Enhanced Surveillance (EHS). ELS has four BDS codes (1.0, 1.7, 2.0, and 3.0) and is used to request information such as call sign or altitude. EHS contains three BDS codes (4.0, 5.0 and 6.0) and provides additional information. The parameters included in these registers are listed in Table 2.3 [9, 17] and will be explained briefly.

BDS register	Parameter
4.0	Selected altitude
	Barometric pressure setting
5.0	Roll angle
	True track angle
	Ground speed
	Track angle rate
	True airspeed
6.0	Magnetic heading
	Indicated airspeed
	Mach number
	Barometric vertical rate
	Inertial vertical velocity

Table 2.3: Content of EHS BDS registers 4.0, 5.0 and 6.0.

The selected altitude can be seen as the target altitude the pilot is flying to. It is based on the barometric altitude, which is the altitude based on air pressure measurements and corrected for the barometric pressure setting. The barometric pressure setting should be the same for all aircraft flying above a certain altitude and differs on lower altitudes depending on the air pressure in an area.

The roll angle is the rotation around the longitudinal axis, which is high if the aircraft makes a steep turn. The track of an aircraft is the path of the aircraft on the ground and the heading is the direction in which the longitudinal axis is pointed. Wind can cause a difference between the heading and track. The true track angle is the angle between the track and the true North, the magnetic heading is the angle between the heading and the magnetic North. The difference between the true and magnetic North is called magnetic declination and changes per location and (slightly) over time.

Ground speed is the speed of the aircraft with respect to the ground, while the true airspeed and indicated airspeed are speeds with respect to the air. The difference between indicated and true airspeed is that the true airspeed is corrected for temperature and pressure altitude. The mach number is another indicator for speed, it

is the speed relative to the speed of sound. Finally, the barometric vertical rate and the inertial vertical velocity are two measures for vertical speed and the basis for the method in this research.

Besides EHS and ELS, a third Mode S service is the interrogation of meteorological reports. The information on turbulence as measured by the aircraft itself can be transmitted through the Meteorological Routine Air Report (MRAR) and Meteorological Hazard Report (MHR). However, in contrast to ELS and EHS, the meteorological reports are not mandated to be transmitted and therefore only a small number of aircraft have transponders that are able to reply to these requests. Conclusion is that MRAR and MHR can be very useful in detecting and measuring turbulence but the information is rarely available [10].

However, turbulence is not only caused by wake vortices. Rising air due to an increase in surface temperature can cause thermal turbulence, air flow hitting obstacles such as mountains can cause mechanical turbulence and sudden changes in wind direction or speed can cause shear turbulence. The method proposed by Olive and Sun does not distinguish between these types of turbulence. Moreover, we are interested in turbulence experienced by approaching air traffic instead of en-route air traffic.

2.3 Approach

An aircraft's descent or approach can be split up in four segments. First the arrival segment, which is the part of descent between cruise and the TMA. Aircraft enter the TMA at an initial approach fix (IAF). At this point, aircraft should have reached flight level 100 or less. Flight level is an aircraft's altitude above sea-level in hundreds of feet. Amsterdam Airport Schiphol has three IAFs: ARTIP, above Lelystad, SUGOL, above the North Sea, and RIVER, above Rotterdam. Once aircraft entered the TMA, they fly the initial approach segment ending at the intermediate fix (IF), followed by the intermediate approach segment ending at the final approach fix (FAF) and the final approach segment. The intermediate approach segment is not always included in the approach procedure, in that case the initial approach segment is followed by the final approach. The final approach segment is the final segment where the aircraft is lined up with the runway for landing.

We will not analyse the entire descent of aircraft but concentrate on the approach in the TMA of Amsterdam Airport Schiphol, starting at one of the IAFs. In particular, focus lies on final approach where separation between aircraft is minimised and RECAT-TBS will be implemented.

Chapter 3

Method and validation

In this chapter, we will explain the method used in this thesis. First, we will explain the algorithm in more detail. Then, we introduce the data used. We will describe the implementation and show the output of the algorithm. Finally, we describe the validation of the algorithm for both en-route and approaching air traffic.

3.1 The algorithm

We use the algorithm to detect and measure turbulence experienced by en-route air traffic based on available Mode S radar data as proposed by Olive and Sun [10]. Parameters in BDS register 6.0 are used. A register which is, in Europe, frequently requested by Mode S radars and frequently transmitted by transponders. The key parameters used for their method are two different sources for vertical speed: the barometric vertical rate and the inertial vertical velocity. The barometric vertical rate is a measure derived from barometer measurements provided by the air data system. The barometer measures air pressure and converts this to an altitude. This altitude is converted to the barometric vertical rate. Due to incomplete filtering it contains significant noise, mainly caused by turbulence [17]. The inertial vertical velocity is computed by the inertial navigation system. This system combines data from multiple sources such as the inertial reference system and the barometric altimeter. The inertial reference system uses signals from gyroscopes and accelerometers to measure the vertical acceleration. Using sensor fusion on the inertial acceleration and the barometer altitude, noises are filtered out and therefore a better estimation of vertical velocity is provided [12].

We use v_b to define the barometric vertical rate and v_i to define the inertial vertical velocity. Noise in v_b differs over time since aircraft experiencing turbulence will show more noise in barometric vertical rate. Therefore, the volatility of v_b and v_i over time

is analysed and the difference in volatility is used as a measure for turbulence. To analyse the volatility, the standard deviation of both parameters is computed over time. The available data is grouped into groups of one minute. In each group j, the standard deviations $\sigma_{v_{b,j}}$ and $\sigma_{v_{i,j}}$ are computed for v_b and v_i, respectively. The absolute difference

$$\Delta\sigma_j = |\sigma_{v_{b,j}} - \sigma_{v_{i,j}}|$$

is used to detect turbulence.

Besides noise differing over time, noise patterns also differ across different aircraft and transponders. Therefore, no general minimum value for $\Delta\sigma_j$ exists that indicates turbulence. For each flight, a threshold is computed using the mean and standard deviation of $\Delta\sigma$, the column containing all $\Delta\sigma_j$. The assumption made is that all aircraft experience some turbulence during their flight and no turbulence will last the entire flight. Based on a large-scale data, the authors define the following threshold:

$$\Delta\sigma_j \geq \overline{\Delta\sigma} + 1.2 \cdot \sigma(\Delta\sigma). \tag{3.1}$$

This means that all values higher than the mean plus 1.2 times the standard deviation are labeled as turbulence.

3.2 Data

For this research, a large amount of data is used. Firstly, multiple data sets containing aircraft and flight information. Secondly, a data set containing reports of wake turbulence encounters. Lastly, multiple data sets containing wind and weather information.

3.2.1 Aircraft data set

The main data used for this thesis is LVNL and contains ARTAS processed surveillance data collected by 15 radars, including radars at Amsterdam Airport Schiphol.

For the analysis of the algorithm, data of flights in an area of approximately 40 kilometers around the Netherlands is used. For the first analysis, seven days of data is made available. The time range of the data is the range from 27-10-2020 12:00:00 to 02-11-2020 23:59:00. This data is mainly used to validate the algorithm.

To be able to distinguish wake turbulence from other detected turbulence, it is useful to analyse situations where pilots reported wake turbulence. Therefore, we have also used data sets containing information on flights at specific dates to analyse these incidents. These specific dates come from the wake vortex reports which will be

explained hereafter. This data is mainly used for the experiments to improve the algorithm.

As mentioned before, the data contains ARTAS processed surveillance data with updates every four seconds. A track that is observed for one hour already leads to 3600/4=900 rows of surveillance information. Besides the required parameters from BDS register 6.0, the data sets contain more columns which will be useful for validating the algorithm and to distinguish wake turbulence. All useful parameters and their units are listed below [4].

1. Time of request (UTC)
2. Latitude (degree)
3. Longitude (degree)
4. Callsign
5. Flight level (25 ft)
6. Magnetic heading (degree)
7. True airspeed (knots)
8. Barometric vertical rate (ft/min)
9. Inertial vertical velocity (ft/min)
10. Roll angle (degree)
11. Track angle (degree)
12. Groundspeed (NM/s)

As we analyse wake vortex effects in approach, we are interested in the sequence in which aircraft landed to know which aircrafts wake vortices might have caused wake turbulence for the trailing aircraft. Since heavier aircraft generate stronger wake vortices than lighter aircraft, this is helpful for analysis of the wake vortex incident. The landing sequence data contains per aircraft landed the date and time of arrival, callsign, aircraft type, WTC, origin of flight, runway where it landed and IAF where it entered the TMA.

In addition to knowing the sequence, the time of arrival is also useful for pre-processing the ARTAS data set. Unreliable measures of barometric vertical rate and inertial vertical velocity measured after landing are included in the data. These measures affect the algorithm, hence need to be filtered out. The time of arrival is used to filter out this unreliable data after landing.

3.2.2 Wake vortex reports

Since we are specifically interested in wake turbulence, it is useful to have data of situations where wake turbulence was reported by the pilot. If pilots believe turbulence is caused by wake vortices, they can report this. For the implementation of RECAT-TBS at Amsterdam Airport Schiphol, LVNL analysed wake vortex incidents reported in 2019. The data used for this research is a summary of their analysis. Note that pilots report wake turbulence if they believe that turbulence was caused by wake vortices. This means that it is still not a hundred percent sure that these situations where indeed the result of wake vortices.

Per incident it contains the date, a short summary of the incident, the runway where the trailing aircraft (should have) landed, the aircraft types, WTC of both leading and trailing aircraft, the distance between and altitude of the aircraft at time of the incident and the intensity. The intensity is estimated based on the pilot report and roll angle and can be weak, moderate or severe depending on the altitude. An equal roll angle can be classified as weak turbulence for higher altitudes while it is classified as moderate turbulence on a lower altitude.

3.2.3 Weather data

To be able to distinguish wake vortex turbulence from other turbulence, for example caused by heavy weather circumstances, we use data provided by LVNL and the Royal Netherlands Meteorological Institute (KNMI). LVNL provided a data set containing wind speed and direction measured, inconsistently, every 30 to 90 seconds per runway. Data provided by the KNMI contains Meteorological Aerodrome Reports (METARs) from Amsterdam Airport Schiphol. A METAR is a weather report formulated by the weather service at an airport every half an hour. It contains coded weather information of for example the wind speed and direction, sight, cloud layers, temperature and rainfall.

3.3 Implementation

The algorithm is implemented in Python. The pseudocode of the algorithm is given in Algorithm 1. The input for the algorithm is a data set as described in Section 3.2.1. Data on many flights is included in the data set. It contains one row per flight per four seconds.

Turbulence is measured per flight, thus the algorithm iterates over all call signs present in the data set. The first step is to filter out outliers from the data by using a moving median. We apply a rolling window of size three, as used by Olive and Sun [10], which means that for every observation, the median of the previous, current and next observation is computed and used.

Next, the data is grouped into groups of one minute. In all groups of one minute, the standard deviation of both v_b and v_i is computed. This results in a data frame containing, for each call sign, one row per minute that the aircraft is observed by the radars. Then, an extra column is created for the absolute difference between these standard deviations, denoted by $\Delta\sigma_j$.

Once all computations in the different groups are done, the turbulence threshold can be computed. Turbulence is detected if $\Delta\sigma_j$ exceeds this threshold.

Algorithm 1 Turbulence

input: data frame D.
output: data frame D' and threshold.
flights $\leftarrow$ all unique call signs
for all call signs **in** flights **do**
  apply moving median to v_b and v_i to filter out outliers
  group data in groups of 1 minute
  for all groups of 1 minute **do**
    $\sigma_{v_{b,j}}$ = standard deviation of v_b in group j
    $\sigma_{v_{i,j}}$ = standard deviation of v_i in group j
    $\Delta\sigma_j = |\sigma_{v_{b,j}} - \sigma_{v_{i,j}}|$
  end for
  compute threshold $\overline{\Delta\sigma} + 1.2\sigma(\Delta\sigma)$
  detect turbulence if $\Delta\sigma_j \geq$ threshold
end for

Plotting the data clearly shows the noise in barometric vertical rate, as shown in the top figure in Figure 3.1 for a flight from Romania to the United Kingdom flying over the Netherlands at October 27, 2020.

As described earlier and also visible in the figure, noise differs over time. Therefore, we analyse the volatility over time by computing the standard deviation in time segments of one minute. The standard deviations are shown in the middle in Figure 3.1. A large peak in the standard deviation of the barometric vertical rate is clearly visible between 13:55 UTC and 14:00 UTC. Moreover, a smaller peak just before 14:24 UTC is observed. To be able to detect turbulence efficiently, the absolute differences between the standard deviations of the barometric vertical rate and the inertial vertical velocity is computed. This is shown in the stemplot in the bottom figure in Figure 3.1. The final step of the algorithm is to compute the threshold as in Equation 3.1. Differences in standard deviations higher than the threshold are labeled as turbulence and are shown in red in the figure.

The data shows a more fluctuating pattern for aircraft in climb or descent. While descending, vertical rate is below zero. An example of this fluctuating pattern is shown in Figure 3.2. What is shown is data of an aircraft starting to descend above the UK, crossing the North Sea and landing at Amsterdam Airport Schiphol. We observe that the threshold for this flight is substantially smaller than the thresholds of the previous shown flight. Hence, smaller differences in variance of v_b and v_i are labeled as turbulence. We conclude that the threshold can differ greatly across flights.

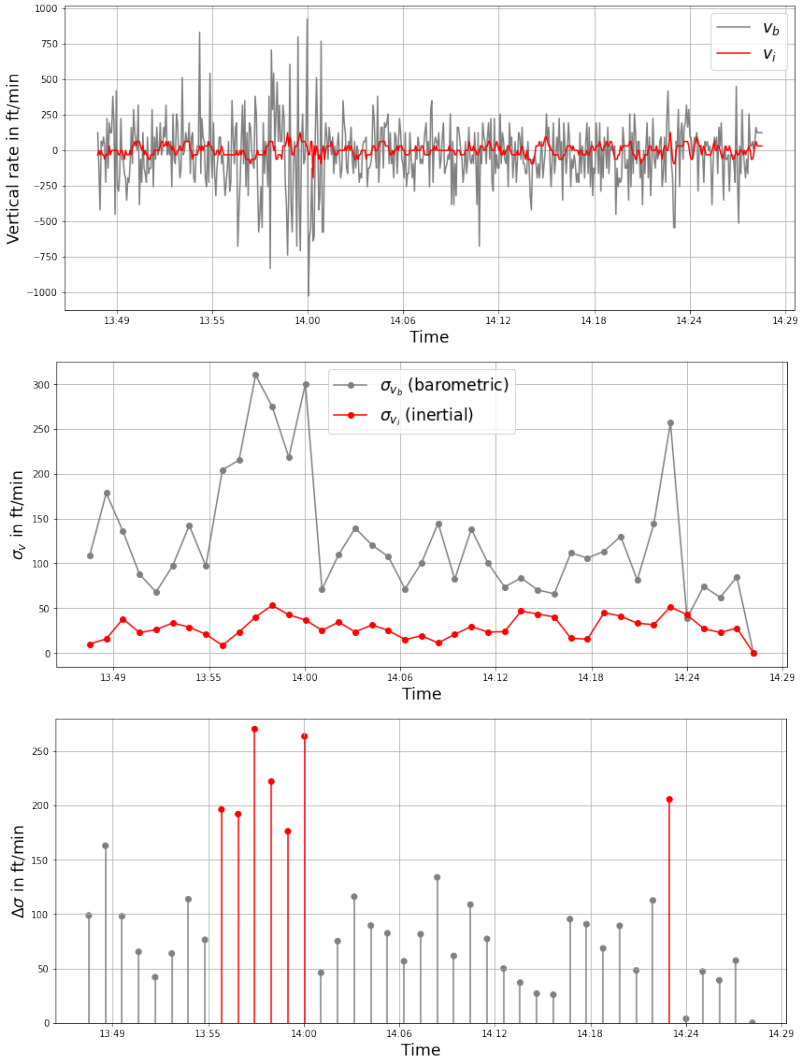

Figure 3.1: Flight from Romania to the UK. Top: two sources of vertical rate. Middle: standard deviations in v_b and v_i in time segments of one minute. Bottom: absolute difference in standard deviation with detected turbulence in red.

Figure 3.2: Descending aircraft. Top: two sources of vertical rate. Middle: standard deviations of v_b and v_i in time segments of one minute. Bottom: absolute difference in standard deviation with detected turbulence in red.

3.4 Validation for en-route air traffic

In this section, we will validate the algorithm for en-route air traffic using different approaches. Where Sun and Olive [10] first validated the method on single flights they boarded themselves, this approach is left out in this research. We validate the algorithm by showing consistent observations by all aircraft and a consistency over time.

3.4.1 Consistency across aircraft

The first validation method is to show that turbulence is observed by all aircraft passing a turbulent area. We will analyse two situations on different days.

First, we will analyse detected turbulence on flights flying over Southern The Netherlands and Western Germany at October 28th 2020 in the morning between 8:30 UTC and 9:00 UTC. The flights flying through this area are plotted in the left of Figure 3.3, with detected turbulence in red. We observe consistently detected turbulence. Note that the algorithm can only detect turbulence in areas where aircraft flew, since aircraft are our data sources. A heatmap based on the average of the turbulence thresholds is produced for an overview of the detected turbulence and is shown on the right of Figure 3.3. The average is computed over all flights crossing a grid cell.

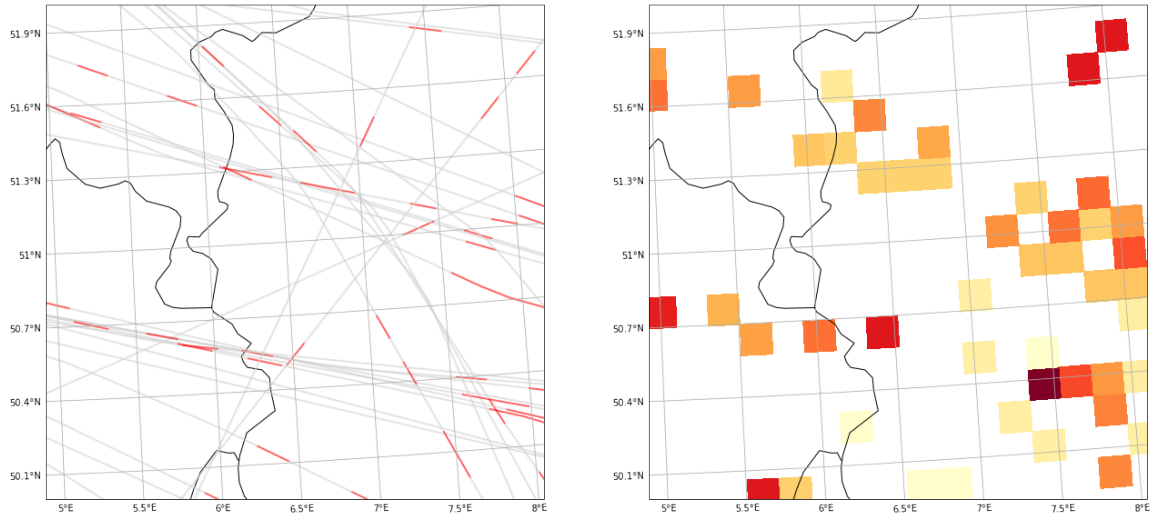

Figure 3.3: Turbulence detected at October 28, 2020 8:30 UTC - 9:00 UTC over Southern the Netherlands and Western Germany. Left: observed flights with detected turbulence in red. Right: heatmap based on average of turbulence thresholds in grid cell.

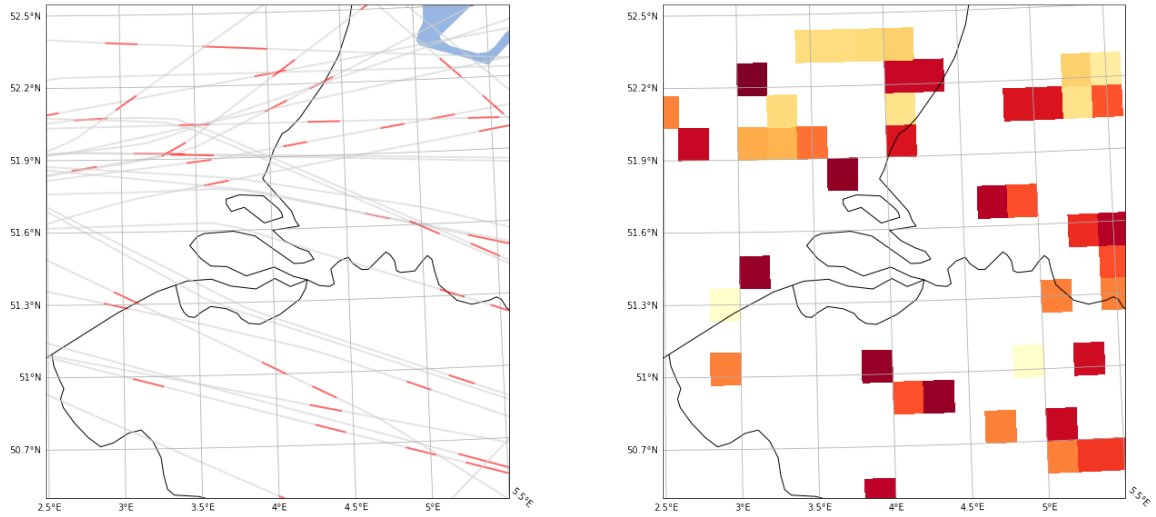

Figure 3.4: Turbulence detected at November 2, 2020 7:00 UTC - 7:30 UTC over Western the Netherlands and Belgium. Left: observed flights with detected turbulence in red. Right: heatmap based on average of turbulence thresholds in grid cell.

Next, we consider a situation at November 2nd 2020 in the morning between 7:00 UTC and 7:30 UTC. We plot flights crossing Western the Netherlands and Belgium during this timeslot together with the detected turbulence. This is shown in Figure 3.4 with the flights in the left figure and the heatmap based on the average of turbulence thresholds in each grid cell in the right figure. Again, we observe consistently detected turbulence for example above the North Sea. We also notice a darker colored heatmap, which means higher turbulence thresholds. The question is whether the height of the threshold values can be used as a measure for the intensity of the turbulence or if, for example, $\Delta\sigma$ works better. It might be aircraft related to have a more noisy barometric vertical rate and therefore a higher threshold. This does not necessarily mean more severe turbulence. We will dive deeper into this in Section 4.1.2.

3.4.2 Consistency over time

The second validation method is to show that turbulence is detected consistently over time. To do this, we analyse flights flying over the Netherlands on two different days.

Figure 3.5 shows four heatmaps of detected turbulence every half an hour from 16:30 UTC to 18:00 UTC on October 27th 2020. For a better overview, we will exclude grid cells where turbulence is detected for only one aircraft from now. Where Sun and Olive [10] conclude consistent turbulence over the Netherlands and Flanders in total, we look at these countries in more detail. In the first two time periods, shown in the

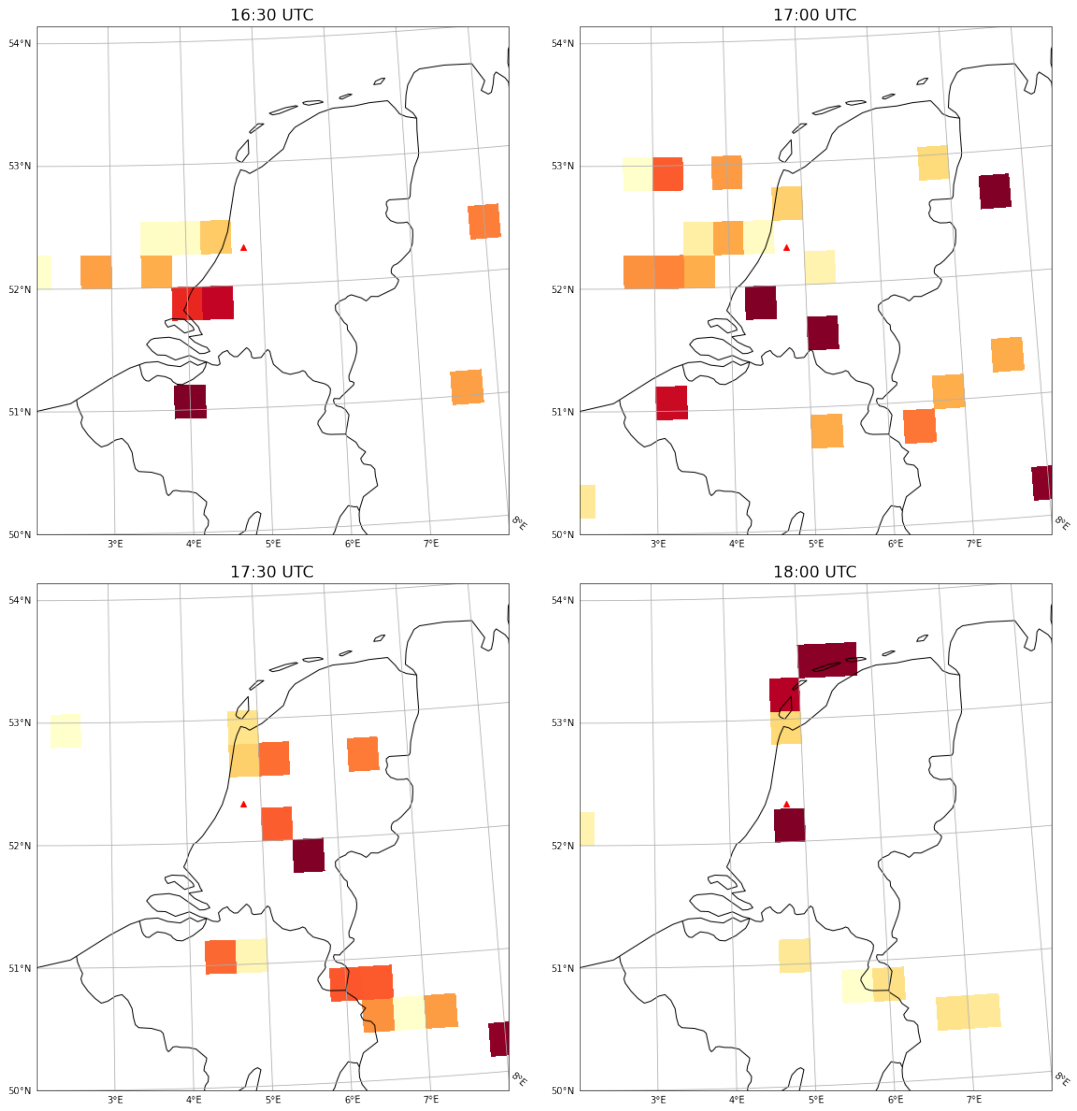

Figure 3.5: Four heatmaps of detected turbulence every 30 minutes at October 27, 2020. Amsterdam Airport Schiphol is indicated with a red triangle.

top two figures, turbulence looks consistent at the Dutch coast, in parts of Germany and below Zeeland, in Belgium. Moreover, in the last two time periods, shown in the bottom two figures, turbulence is consistently detected around the South of the Netherlands, in the middle of Belgium and around Amsterdam. However, we should keep in mind that aircraft are the sensors which means that turbulence can only be detected in areas where aircraft have passed. So, it does not mean that turbulence above the North Sea was not there in the last two time periods since it is possible

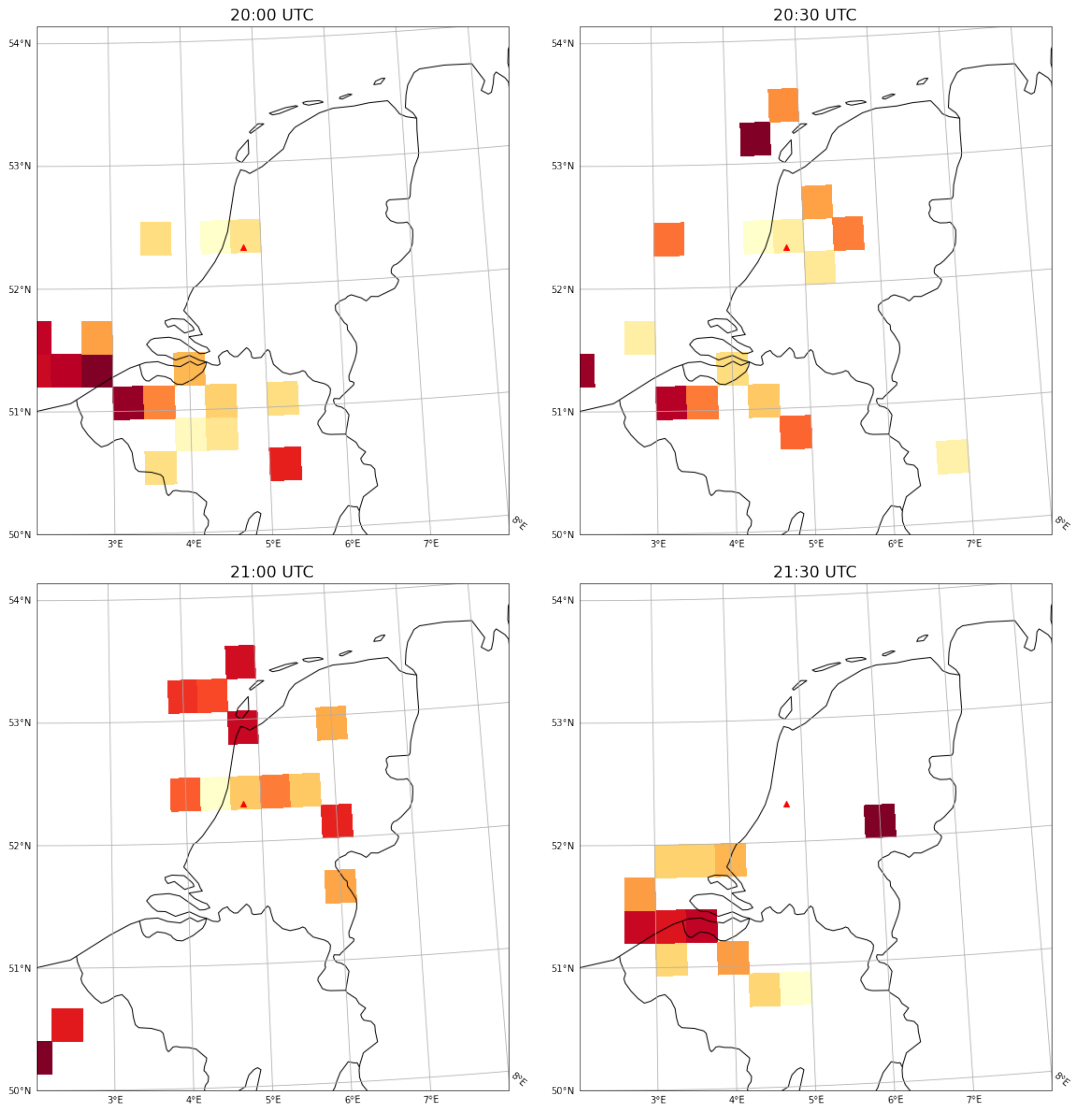

Figure 3.6: Four heatmaps of detected turbulence every 30 minutes at October 31, 2020. Amsterdam Airport Schiphol is indicated with a red triangle.

that there where no, or less, flights in that area.

Next, we analyse the consistency over time at October 31st 2020. We analyse flights in the same bounding box around the Netherlands as before. Heatmaps of detected turbulence every half an hour between 20:00 UTC and 21:30 UTC are shown in Figure 3.6. We observe much turbulence in and below Zeeland. However, this turbulence is not clear in the bottom left figure. Analysing the tracks of the flights clarifies that

there were less flights in this area around 21:00 UTC. Flights that passed Zeeland did however experience turbulence, but since we excluded grid cells where turbulence is detected for only one aircraft this is not visible in the figure. Besides this, turbulence is also consistently detected around Amsterdam and, for a shorter period, above the islands.

3.5 Validation for approaching air traffic

In this section, we will validate the algorithm for air traffic in the approach area. As mentioned before, we will not analyse the entire descent but focus on the approach in the TMA of Amsterdam Airport Schiphol. Hence, focus lies on the last 100 flight levels (100.000 feet) of descent. We have seen that the algorithm shows consistency across aircraft and over time for en-route air traffic. For aircraft in cruise, the vertical rates fluctuate around zero whereas in approaching air traffic the vertical rates do not fluctuate around a specific value, as we have seen in Section 3.3. The question is whether the algorithm still detects turbulence correctly in this case and if it is possible to detect and distinguish wake turbulence. We validate the algorithm by showing consistent observations by all aircraft, a consistency over time, a consistency with wind fields and a consistency with reported wake turbulence encounters.

3.5.1 Consistency across aircraft

The first validation method is, similar as for en-route air traffic, to show that turbulence in an area is observed by all aircraft passing it. We will analyse two approach situations at the same time on a different day.

First, we analyse a situation on a summer day in 2019. We plot approaching flights that have landed between 10:30 UTC and 11:00 UTC and color detected turbulence in red. This is shown in Figure 3.7. The three IAFs can be recognized. We observe consistently detected turbulence for example above the North Sea. Moreover, much turbulence is detected in the final turn when aircraft turn to final approach.

Next, we analyse approaching air traffic on a winter day in 2019. We plot approaching flights that have landed between 10:30 UTC and 11:00 UTC. The flights are shown in Figure 3.8, with detected turbulence in red. As before, we observe turbulence detected at some aircraft when turning to their final approach. Also, multiple aircraft experience turbulence in the final moments before landing.

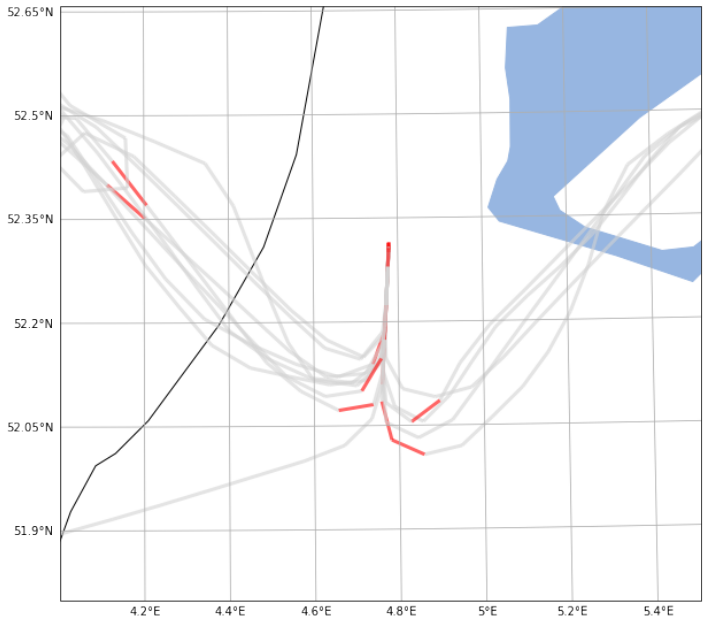

Figure 3.7: Turbulence detected on a summer day in 2019, between 10:30 UTC and 11:00 UTC. Detected turbulence in red.

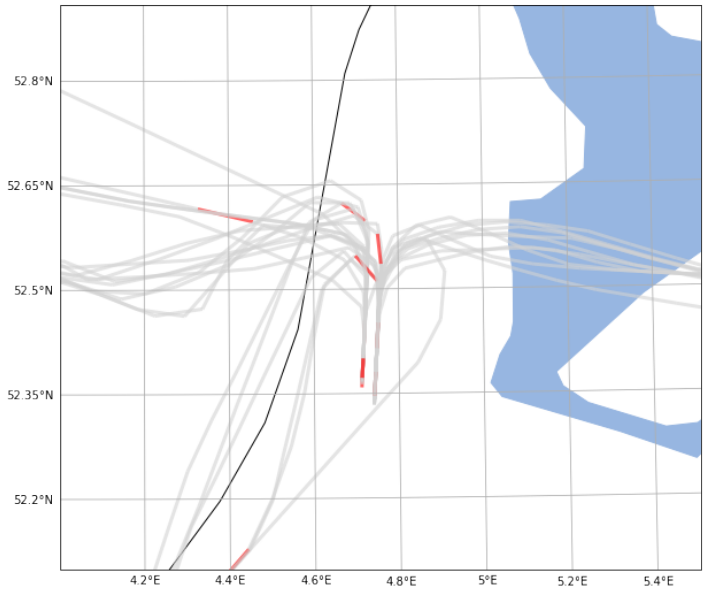

Figure 3.8: Turbulence detected on a winter day in 2019, between 10:30 UTC and 11:00 UTC. Detected turbulence in red.

3.5.2 Consistency over time

Next, we check if the algorithm detects turbulence consistent over time. We analyse approaching air traffic in four consecutive time periods of 15 minutes. The plots of the tracks are shown in Figure 3.9, with detected turbulence in red. We observe an increase in detected turbulence over time. Turbulence in the final moments before landing is observed consistently. Moreover, turbulence detected in the turn to final approach is observed consistently after 9:45 UTC. However, due to the multiple turbulent moments detected in single time periods, we cannot conclude a clear consistency over time.

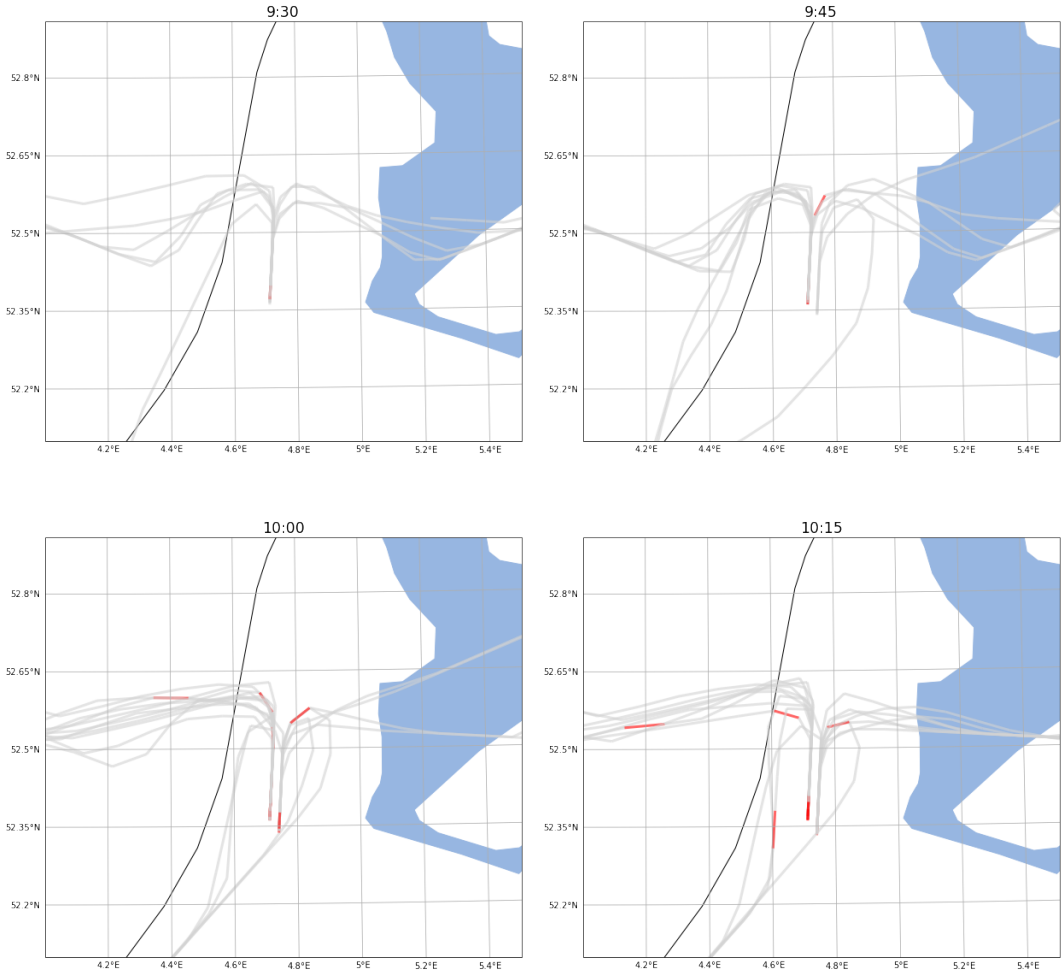

Figure 3.9: Four track plots of approaching air traffic in consecutive time periods, detected turbulence in red.

We analyse the same time periods on another day. The tracks are plotted and shown in Figure 3.10. The consistency over time is even less visible in this example. We conclude that for approaching air traffic less consistent turbulence is detected over time when compared to en-route air traffic. Turbulence detected on lower altitudes might be less time consistent, hence not detected by the algorithm. As we cannot validate the algorithm using this method, we will use two other ways.

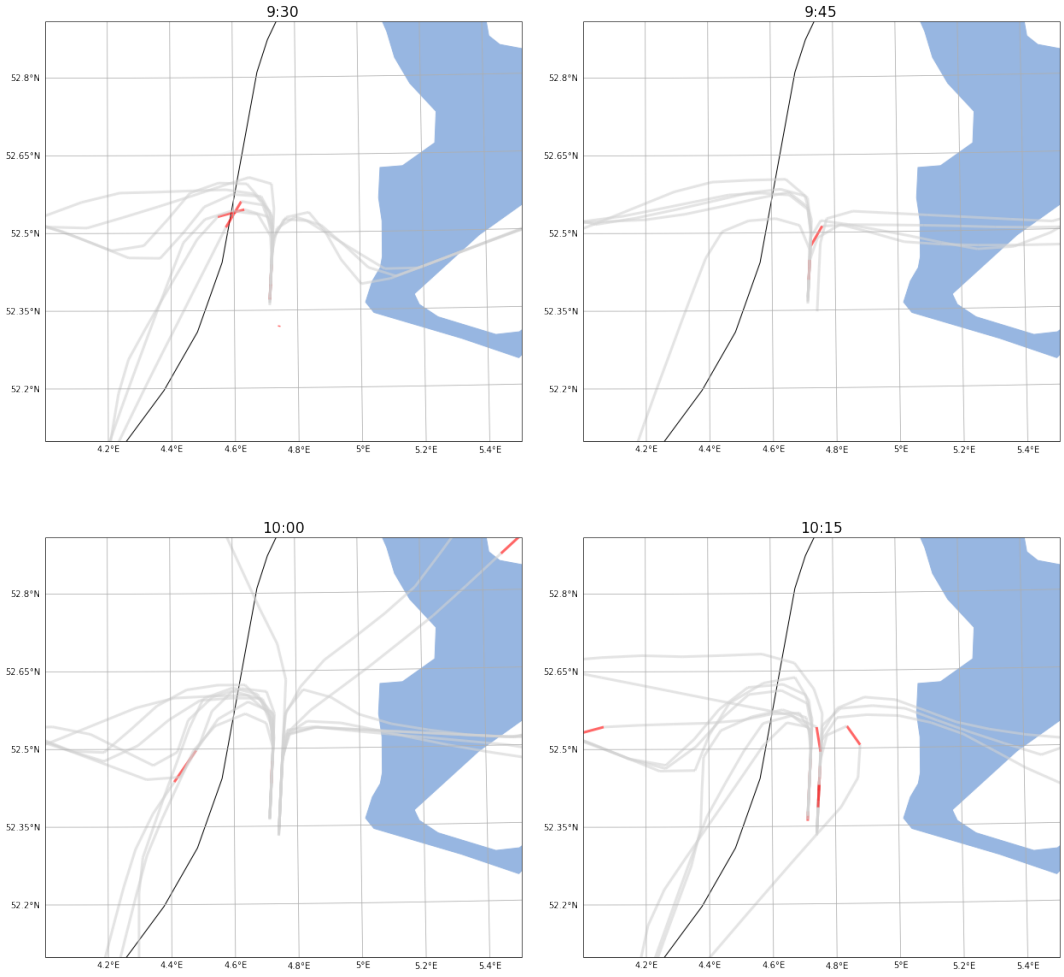

Figure 3.10: Four track plots of approaching air traffic in consecutive time periods, detected turbulence in red.

3.5.3 Consistency with weather effects

In heavy wind we expect aircraft to experience more turbulence than if there is little wind. We will analyse a situation where aircraft landed in heavy wind and compare it to a situation where aircraft landed with little wind and see if the algorithm indeed detects more turbulence in the first situation. In Figure 3.11, aircraft approaching in the same time period on a different day are plotted. Most of the flights landed on both days, which makes it possible to compare these two situations. The left figure shows flights that landed in little wind with a windspeed of approximately eight knots, with turbulence detected by the algorithm in red. We observe a little turbulence detected in the beginning and at the and of final approach. In the right figure, flights that landed in heavy wind of approximately 30 knots are shown. Much turbulence is detected in their final approach. Also, one flight executed a go around, which means that the landing is aborted, likely because the heavy wind made it impossible to land safely. The expected more turbulence in heavy wind situations is confirmed by this example.

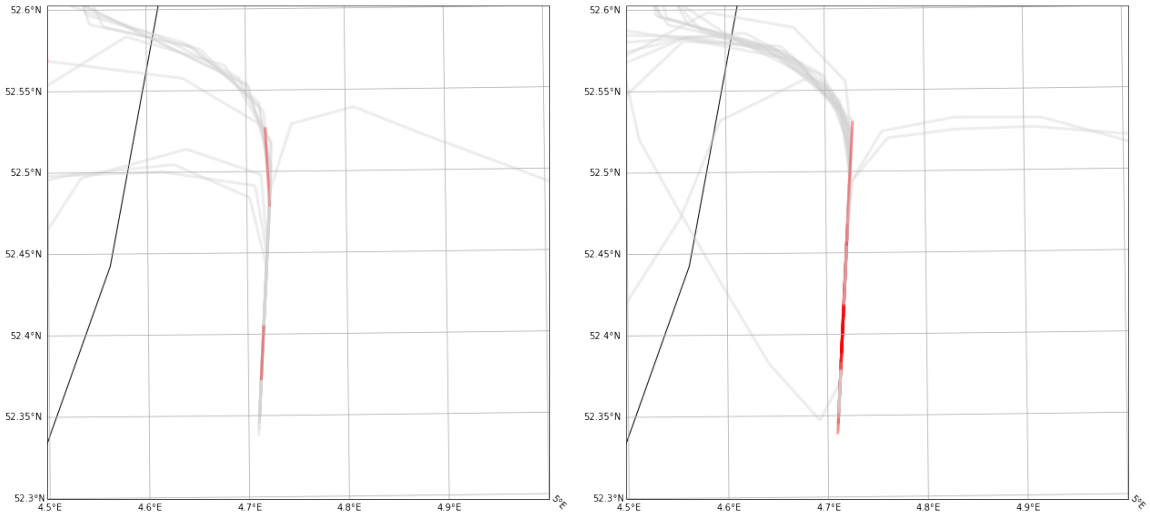

Figure 3.11: Left: little turbulence detected for aircraft landing with little wind. Right: much turbulence detected for aircraft landing in strong wind.

Also, aircraft flying through clouds can experience quite some turbulence. We analyse a situation where clouds were reported by the METAR of Amsterdam Airport Schiphol between 1800 and 2300 feet. The result of the algorithm on approaching air traffic in this situation is shown in the left figure in Figure 3.12. We observe much turbulence in the turn to final approach, where most aircraft have an altitude between 3000 and 1000 feet. This is in line with the reported clouds.

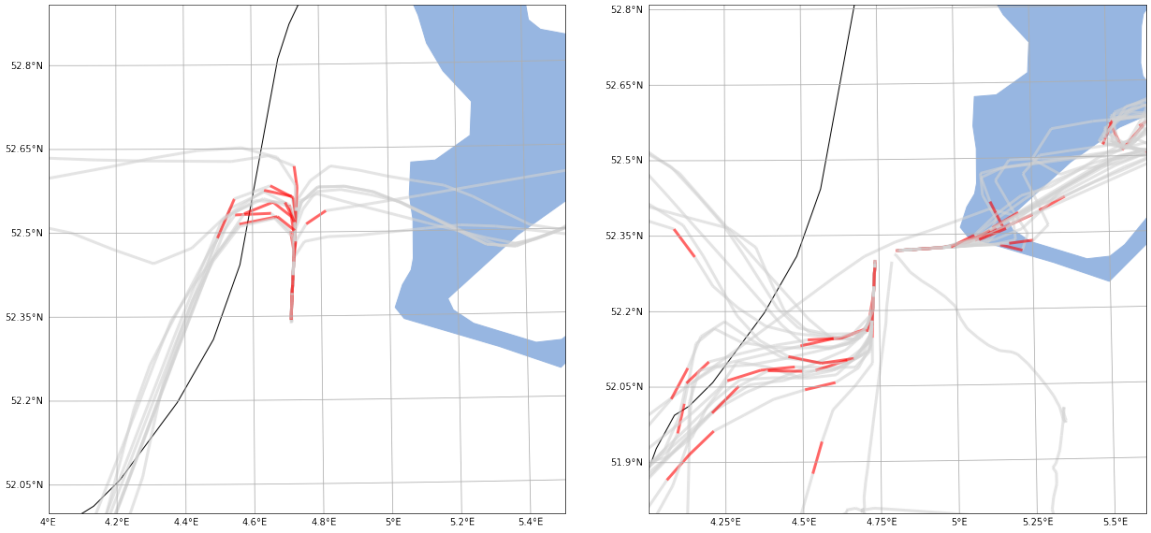

Figure 3.12: Left: approaching air traffic in a time period where clouds were reported. Right: approaching air traffic in a time period where rain was reported.

Finally, we investigate a situation where rain and wind with a speed of approximately seven knots were reported by the METAR of Amsterdam Airport Schiphol. The plot of approaching aircraft in this time period of 30 minutes is shown in the right figure in Figure 3.12. Clearly, clouds are also present in this situation. We observe much turbulence, which is likely to be caused by the clouds, wind and/or rain.

3.5.4 Consistency with wake vortex reports

Since we are mainly interested in wake turbulence, we will analyse situations where wake turbulence is reported by the pilot and of which we are sure turbulence is experienced by aircraft. As mentioned before, for each reported wake turbulence situation, we have the callsigns of involved aircraft, the distance between the two aircraft and the altitude of the trailing aircraft at time of the incident. We use this information to identify the wake vortex incident in the data set and see if the algorithm detects the reported turbulence.

We will analyse two situations. First, we analyse the approach of a flight where wake turbulence was reported by a medium aircraft around flight level 70. We run the algorithm on the available data of this flight and analyse the barometric vertical rate and inertial vertical velocity and the outcome of the algorithm. This is shown in Figure 3.13. The first figure plots the barometric measure v_b and the inertial measure v_i. Noise in the barometric measure is clearly visible in the end of descent

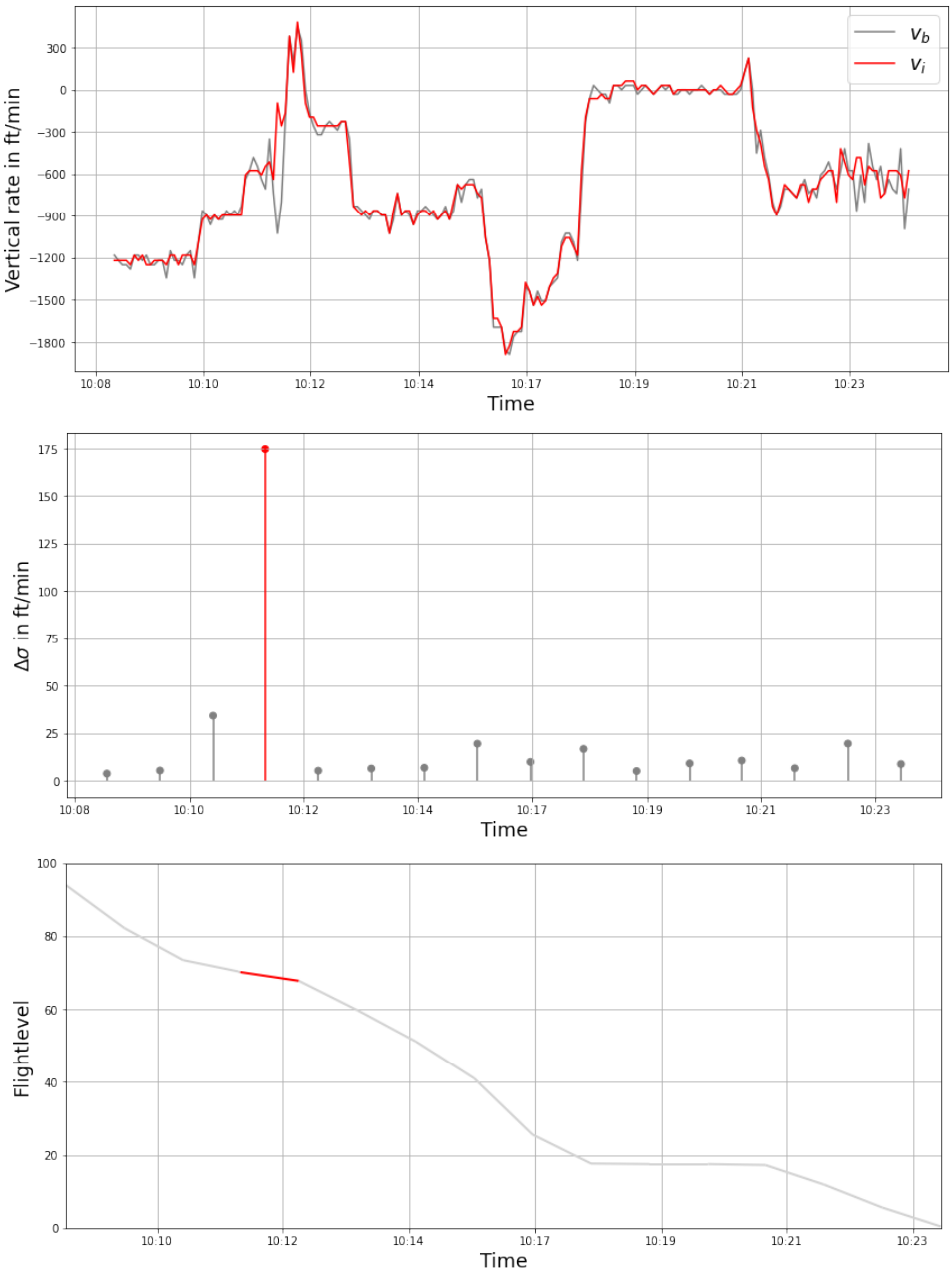

Figure 3.13: Consistency with wake vortex report. Top: two sources of vertical rate. Middle: absolute difference in standard deviation. Bottom: flight level with detected turbulence in red.

and also between 10:10 UTC and 10:12 UTC. The second figure shows the difference in standard deviation, computed per minute and with detected turbulence in red. The algorithm detected turbulence around 10:12 UTC. The bottom figure shows the altitude of the aircraft in flight levels over time. The time segments where turbulence is detected are colored red. We observe that the detected turbulence occurred around flight level 70, which corresponds to the wake vortex report. The aircraft in front was a heavy aircraft and the aircraft were 7.8 NM separated, well above the separation minimum of 5 NM. Whether this turbulence was caused by a wake vortex or not, turbulence was reported by the pilot and the algorithm detected turbulence where it should have.

The second situation we analyse is a situation where wake turbulence was reported by the pilot flying a medium aircraft in final approach below 1000 ft. We plotted the barometric and inertial measures for this situation and ran the algorithm. The results are shown in Figure 3.14. The algorithm detected turbulence around 10:20 UTC when the aircraft was in its final approach, corresponding to the wake vortex report. We observe that the aircraft aborted the landing. The pilot probably experienced too much turbulence to land safely and executed a go around. According to the algorithm, it landed without turbulence the second time.

However, there are also situations where the algorithm does not detect turbulence at times when wake turbulence is reported and noise in the barometric vertical rate is visible. Also, we have seen huge differences in threshold value for different aircraft. These differences are not only visible for different aircraft, but also for same types of aircraft on different days or routes. To analyse wake turbulence encounters, being able to compare the intensity of turbulence could be helpful. Since the threshold seems not to be a good measure for this, we might want to investigate if $\Delta\sigma$ is. Lastly, we have seen much turbulence being detected in heavy weather circumstances. If we want to get insight in the number of wake turbulence encounters, we should be able to distinguish wake turbulence from other turbulence. We will elaborate on these shortcomings in Chapter 4.

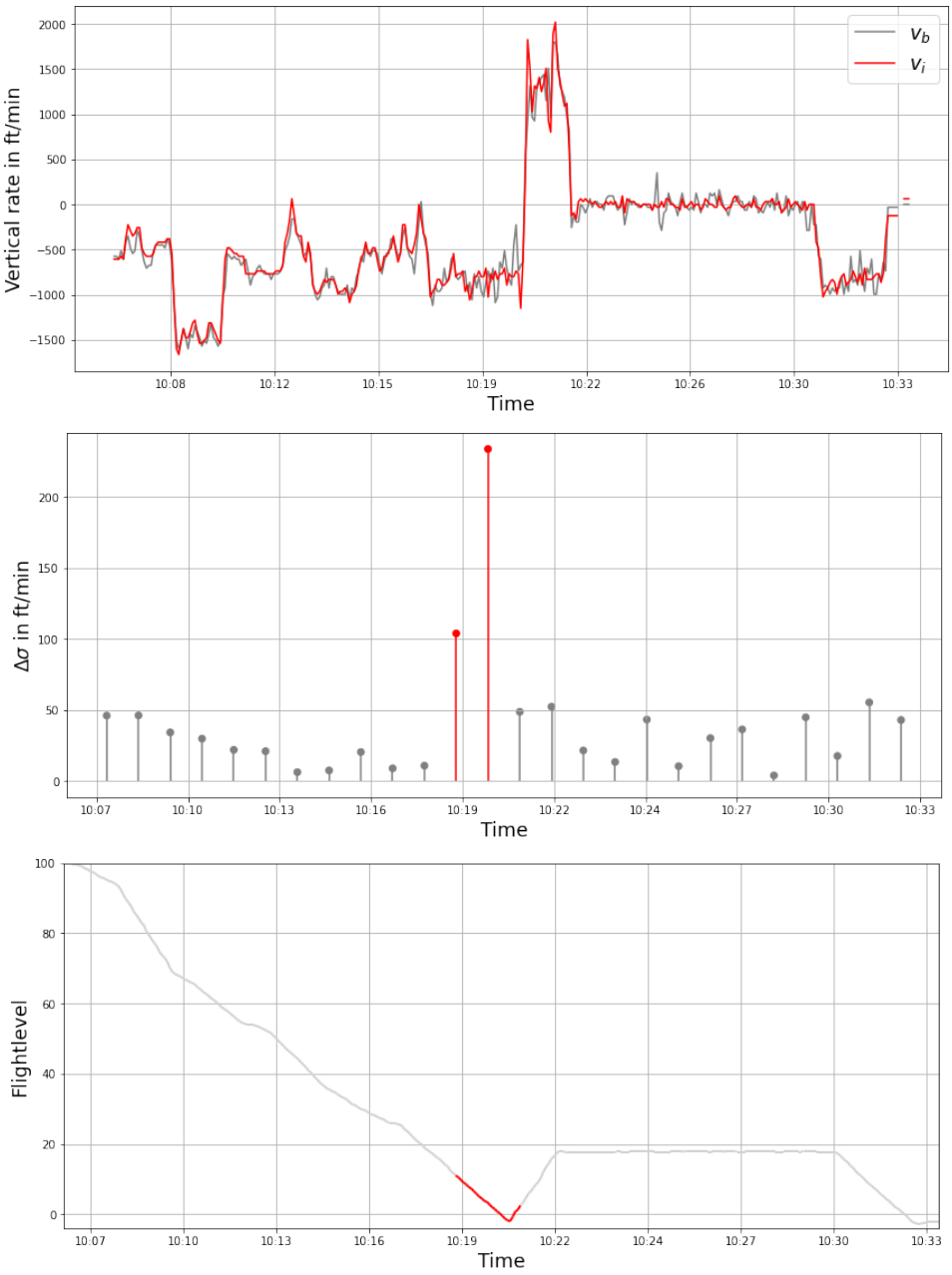

Figure 3.14: Consistency with wake vortex report. Top: two sources of vertical rate. Middle: absolute difference in standard deviation. Bottom: flight level with detected turbulence in red.

Chapter 4

Experiments and results

During the validation of the algorithm we have come across some problems. Firstly, not all known wake turbulence encounters are detected by the algorithm, while noise in the barometric vertical rate is visible. Also, thresholds differ a lot, among different aircraft and routes but also among days or times for the same aircraft and route. This makes it hard to decide on the intensity of turbulence which would be helpful when analysing wake vortex encounters and is one of the goals of the research. We will propose adaptations to the current algorithm to solve these problems in Section 4.1. Besides the already mentioned limitations of the algorithm, another problem is that the algorithm detects more than only wake turbulence. We will analyse turbulence on final approach in situations where weather could not have been a cause in Section 4.2.

4.1 Algorithm optimization

In this section, we will propose adaptations to improve the algorithm. First, we discuss how we can improve the detection of turbulence by the algorithm by three methods. Then, we will propose a method to be able to compare intensities of different turbulence encounters.

4.1.1 Improve turbulence detection

There are examples where wake turbulence is reported by the pilot and noise is visible in the barometric vertical rate, but the algorithm does not detect them. The question is where in the algorithm this happens. It might be caused by grouping the data into time segments of one minute or the peaks in barometric vertical rate might be filtered out as outlier when applying the moving median. Another option is that an aircraft

measured heavy noise during cruise, causing the threshold to be high, resulting in moderate noise not being detected. We will discuss all these options.

Moving standard deviation

Using the original algorithm, only 43.8% of the reported wake turbulence encounters are detected. Noise in the barometric vertical rate is visible in most of these cases, but this information seems to disappear during the algorithm. An important step in the algorithm is that the data is grouped into segments of one minute. Within these segments, standard deviations are computed and used for turbulence detection. A positive aspect of this is that the amount of data is reduced to one row of data per minute instead of one row every four seconds. However, lots of information is lost. A peak in the data happening at the split of time segments causes only half of the peak values to be considered in each time segment. Hence, the standard deviations in both time segments will be lower than if the peak would have been entirely within one time segment. A lower standard deviation of the barometric vertical rate results in a lower $\Delta\sigma$, which causes the algorithm to be less likely to detect the moment with noisy barometric vertical rate as turbulence.

As a solution to the above shortcoming we propose using a moving standard deviation with a window size of one minute. This means that the standard deviation is computed for every possible window of one minute. If a peak is at the split for one window, it will be completely within one of the next windows and still be detected. An example where pilot-reported wake turbulence is not detected is shown in Figure 4.1. The final 100 flight levels are analysed. The top figure shows the barometric vertical rate and the inertial vertical velocity. The figure in the middle shows the standard deviations of both parameters in time segments of one minute. The obtained result is shown in the bottom figure. No turbulence is detected by the algorithm here. In Figure 4.2, the moving standard deviation is used. The top figure shows the moving standard deviation for both the barometric as the inertial measure. The figure in the middle plots the difference between the standard deviations with values above the threshold in red. The threshold is computed as before as in Equation (3.1), now taking the mean and standard deviation over many more values. We observe that between 11:11 UTC and 11:12 UTC the algorithm detected turbulence, where it did not detect any turbulence before. As mentioned before, the wake turbulence encounter was reported at approximately flight level 45. The bottom figure in Figure 4.2 shows that the algorithm indeed detected turbulence at this altitude. So, the moving standard deviation makes it possible to detect wake turbulence reported by the pilot that the original algorithm did not detect.

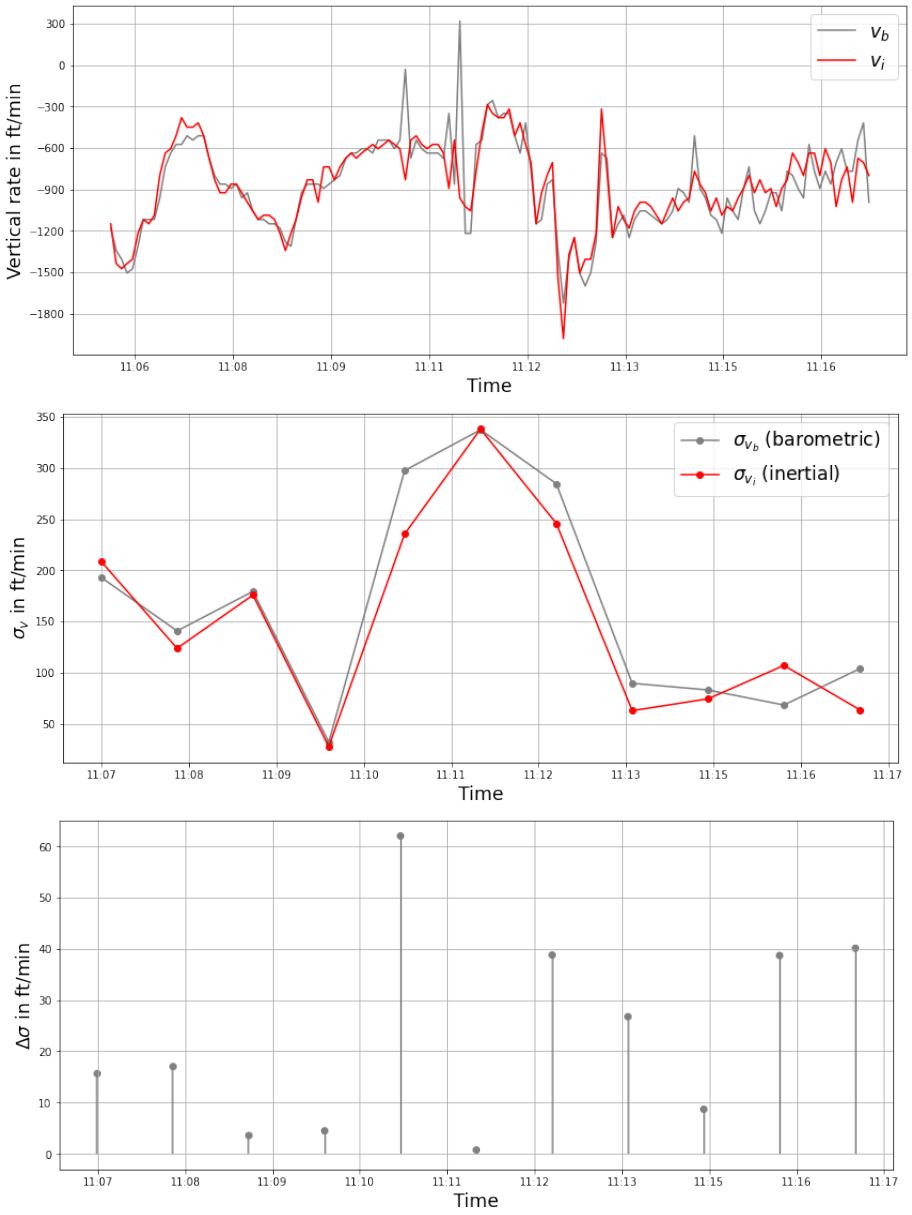

Figure 4.1: Turbulence not detected using the original algorithm. Top: two sources of vertical rate. Middle: standard deviations of v_b and v_i in time segments of one minute. Bottom: absolute difference in standard deviation with detected turbulence in red.

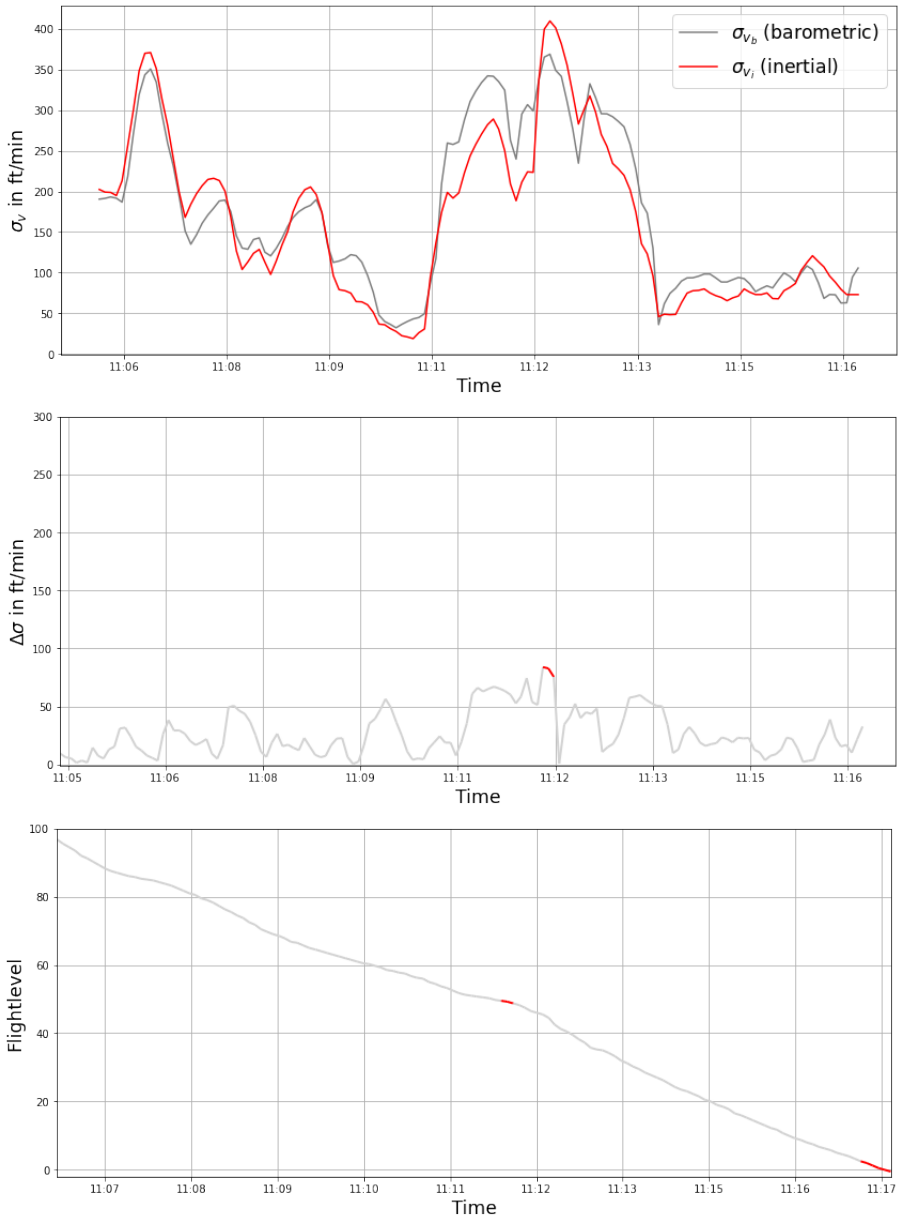

Figure 4.2: Turbulence is detected using improved algorithm. Top: two sources of vertical rate. Middle: standard deviations of v_b and v_i in time segments of one minute. Bottom: absolute difference in standard deviation with detected turbulence in red.

A second advantage of the moving standard deviation is that turbulence is detected more precisely. If turbulence was detected by the original algorithm, we knew that somewhere in that time segment of a minute the barometric vertical rate has been very noisy compared to the inertial vertical velocity. If the noise in the data is at a split of time segments and therefore present in both time segments for a few seconds, both time segments could have a $\Delta\sigma$ above threshold due to this peak. If this happens, the algorithm detects turbulence for two minutes long while it could have been only 20 seconds.

An example is shown in Figure 4.3. The result of the algorithm using a moving standard deviation is shown in a plot of the flight level over time. A wake vortex encounter was reported by the pilot in the final approach, below an altitude of 1000 ft. We observe turbulence detected at this point, just before the planned landing. However, due to this turbulence the aircraft decided not to land and execute a go around, which is not entirely visible in the figure. Note that the detected turbulence lasts a lot shorter than a minute.

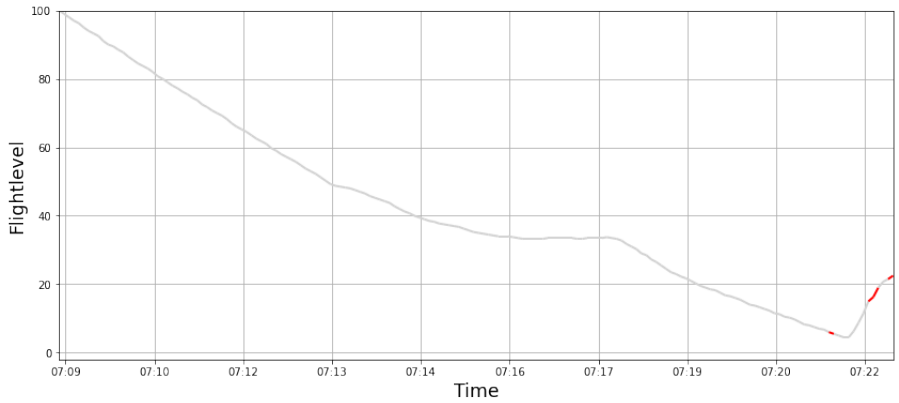

Figure 4.3: An example of a more precise turbulence detection. The result of the algorithm is shown on a plot of flight level over time, wake turbulence detected around 7:21 UTC.

On a large scale, we would still like to have turbulence detected consistently by all aircraft. In Figure 4.4, we plotted approaching aircraft flying through a layer of clouds. This example is similar to Figure 3.12, now using the moving standard deviation. We observe that turbulence at the height of the clouds is detected even more consistently by all aircraft than with the original algorithm. Also important is that there are large parts of the flights turbulence free for all aircraft.

In Figure 4.5, approaching air traffic is shown in a situation that we have not seen before. Few clouds around 4000 feet were reported in the METAR of Amsterdam

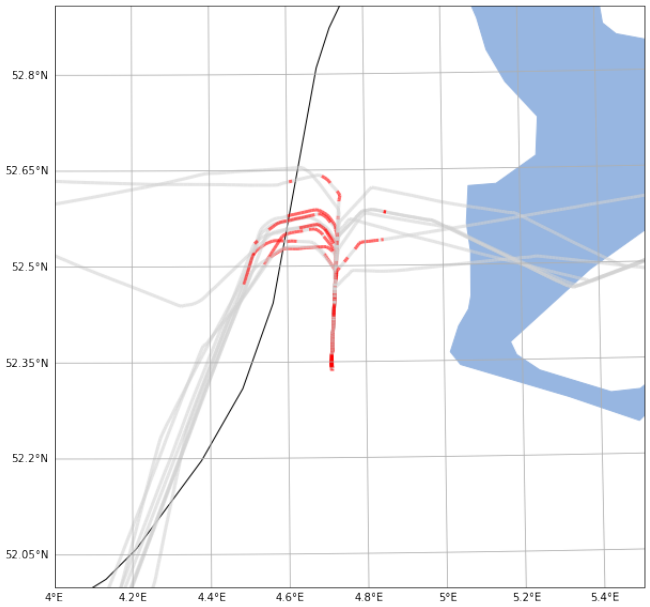

Figure 4.4: An example of the algorithm using a moving standard deviation on a larger scale.

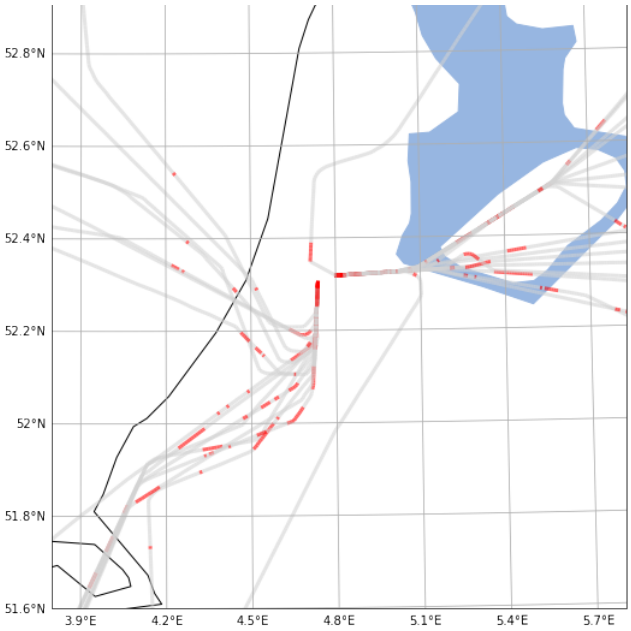

Figure 4.5: An example of the algorithm using a moving standard deviation on a larger scale.

Airport Schiphol. We observe some consistent detected turbulence on flights entering the TMA at RIVER and also above Flevoland, likely to be caused by the clouds. Moreover, multiple aircraft have turbulence detected on final.

Besides the consistently detected turbulence, we also observe many small and short lasting turbulent periods to be detected. This might have been turbulence, but the question is whether these detections are useful or only making the output unclear. As we have seen in the example in Figure 4.3, these short lasting turbulent periods can indeed indicate wake turbulence. But, it could also be the case that not all outliers are filtered out by the algorithm when applying the moving median and that these short lasting noisy peaks are still outliers and not turbulence.

Implementing the moving standard deviation in the algorithm makes it possible to detect 68.8% of the reported wake turbulence encounters. Half of the extra detected cases are reported in final approach. Since wake turbulence is detected on final approach using the moving standard deviation that was not detected by the original algorithm, we conclude that it is an improvement to the algorithm. However, we will not focus too much on the short lasting turbulent moments in the initial approach. Some of the reported cases that are still not detected do show significant noise in barometric vertical rate. The cases that are not detected that do not show significant noise in barometric vertical rate are mostly weak reported wake turbulence encounters. An overview of the results of the original algorithm and the proposed improved algorithm is shown in Table 4.1, where the results are split up in results for encounters on final approach and encounters on higher altitudes in initial approach. In total 62.5% of the reported wake turbulence encounters are on final approach.

	Original algorithm	Improved algorithm
Final approach	40%	60%
Initial approach	50%	66.7%
Total	43.8%	68.8%

Table 4.1: An overview of the percentages of algorithm detections per approach segment.

Descent only

The more heavy noise in barometric vertical rate during the flight, the higher the threshold and the less likely weaker noise will be seen by the algorithm. However, this weaker noise might be caused by a wake vortex and therefore is preferred to be detected. Besides some perfectly detected wake turbulence, we have some examples of wake vortex reports that are not detected by the algorithm. We propose to analyse

only data where the aircraft was in descent and not take into account the en-route part of the flight. In this way, we might filter out some heavy noise and base the threshold on the average level of noise in descent only. By doing this, we ignore the assumption made by Olive and Sun [10]. They assume that this threshold works well because an aircraft will always experience turbulence during a flight and this turbulence will never last the entire flight. If we use descent data only, we change this assumption to the assumption that all aircraft experience some turbulence during descent, which is less true.

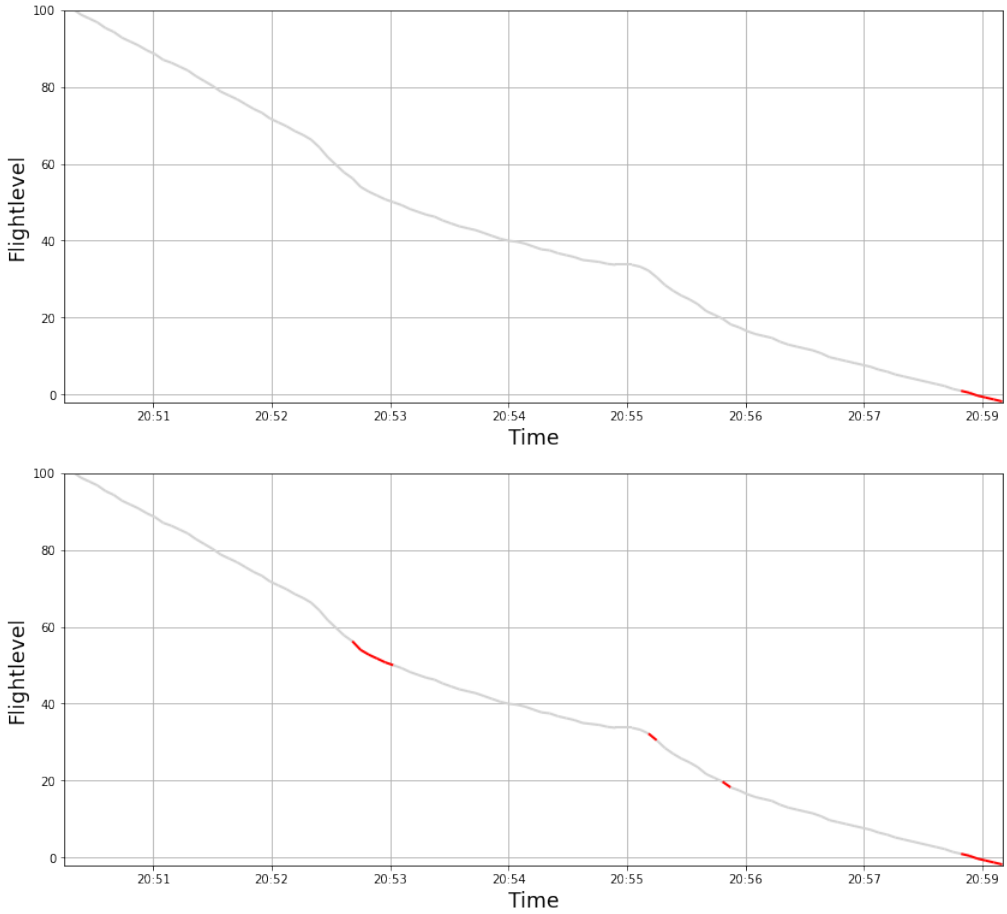

Figure 4.6: Top: result using all data, reported wake turbulence not detected. Bottom: result using descent data only, reported wake turbulence detected around flight level 20.

We will analyse a flight where wake turbulence was reported, but not detected by the algorithm. Weak wake turbulence was reported at flight level 20. Figure 4.6 shows

the results of the algorithm on the plot of the flight level over time with detected turbulence in red. The top figure is the result when running the algorithm on all data of this flight, the result in the bottom figure is obtained when descent data is used only. The turbulence in the final minutes of the flight is the only turbulence detected when using all data. When the algorithm is run on the descent data only, three more periods with turbulence are detected. And, fortunately, one of those moments is at flight level 20, the altitude at which wake turbulence was detected. In this case, reducing the data resulted in a lower threshold causing more periods to be labeled as turbulence. However, it can also increase the threshold if descent had on average more noise in barometric vertical rate. This might cause originally detected turbulence, not to be detected anymore.

Since this was an example of a wake turbulence encounter reported as weak, this supports the idea that $\Delta\sigma$ could be a measure for the strength of turbulence. Namely, this weak turbulence resulted in a low $\Delta\sigma$, smaller than the threshold that was originally used. We will elaborate more on this in Section 4.1.2.

For the algorithm to run on descent data only we conclude that it will work in some situations but, holding on to the assumption made by Olive and Sun, it is not a good solution on the large scale.

Extra radar data

We still have cases where the algorithm did not detect turbulence where wake turbulence was reported by the pilot. We take a look at the barometric vertical rate, v_b, and inertial vertical velocity, v_i, of one such example, shown in the top figure in Figure 4.7. We observe a very noisy barometric vertical rate from 11:57 UTC till 12:14 UTC. This happened when the flight was in cruise, as can be concluded from the vertical rate fluctuating around zero. Later on, around 12:34 UTC, a huge peak in barometric vertical rate is visible. In the bottom figure in Figure 4.7, the result of the algorithm is shown on a plot of the flight level over time. The algorithm detected turbulence in cruise but the peak at 12:34 UTC is not seen. Moderate wake turbulence was reported around flight level 70, which seems to be, when combining the two figures, exactly at the peak. Since it is a very short lasting peak, it might have been removed when executing the moving median to filter out outliers and therefore not detected as turbulence. This is confirmed in Figure 4.8, where v_b and v_i are plotted after removing the outliers. Since we know that the aircraft experienced turbulence around 12:34 UTC, more data around that time could prevent the peak from being removed.

The data set we have used so far is ARTAS processed surveillance data. Every four seconds, it adds the most recent information collected by one of the radars. This

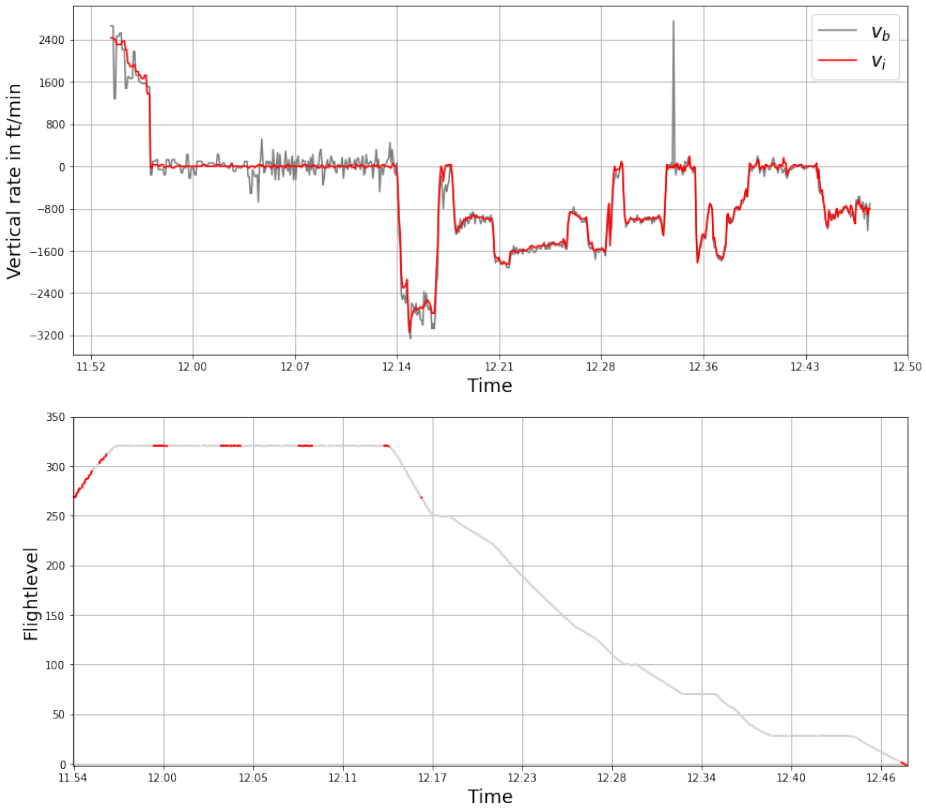

Figure 4.7: An example where wake turbulence is not detected with ARTAS data. Top: barometric vertical rate shows peak around 12:35 UTC. Bottom: result of the algorithm plotted on flight level over time.

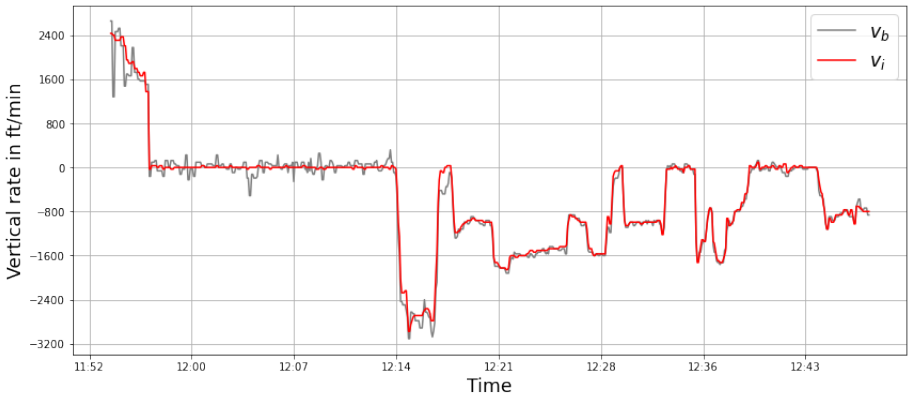

Figure 4.8: Two sources of vertical rate after filtering out outliers.

means that many useful radar data is lost. This data might prevent turbulence to be removed as outlier or introduce very new peaks in barometric vertical rate. Therefore, we will merge the ARTAS data set with raw Mode-S radar data obtained from 3 of the 15 radars. The three radars used are radars around Amsterdam Airport Schiphol: TAR-I, TAR-West and Soesterberg. Since the radars request information at different moments in time, this extends the data set to a data set with more updates than only every four seconds.

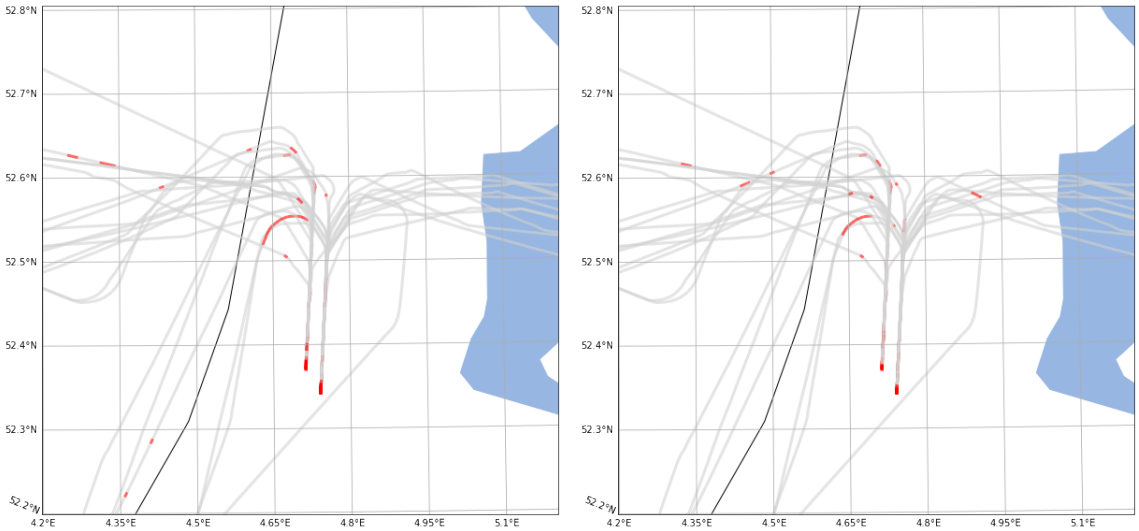

Figure 4.9: Result of the algorithm when excluding the extra radar data on the left compared to the result when including the extra radar data on the right.

In Figure 4.9, the result of the algorithm using data excluding this extra radar data in the left figure is compared to the result of the algorithm using data including it in the right figure. The figure shows aircraft approaching Amsterdam Airport Schiphol between 10:30 UTC and 11:00 UTC. We observe extra cases of turbulence being detected, but also cases of turbulence that disappeared. This may indicate a more precise turbulence detection.

We return to the example from Figure 4.7 and now use the extended data set. The barometric vertical rate and inertial vertical velocity are plotted in Figure 4.10, together with the algorithm result on the flight level. We do observe an extra peak around 12:34 UTC, but unfortunately it is still removed as outlier and therefore not detected as turbulence. However, using this extended data set causes extra moments to be detected as turbulence in cruise and in the beginning of descent.

Including extra radar data does not make a difference for the wake turbulence encounters that we consider in this research. Filtering out outliers causes these cases of

turbulence to be filtered out, even with extra data included. An option is to skip the filtering, however this leads to possible false positives. The algorithm already showed that it is able to detect many true wake turbulence encounters. Only a few more are detected when skipping the outlier filtering. However, many other possibly false positives are detected causing unclear results. Therefore, we conclude that skipping the outlier filteringwill not improve the analysis of wake turbulence encounters. However, although including the extra radar data did not show extra reported wake turbulence to be detected it gives a more precise result and can be useful for detecting wake turbulence on a large scale.

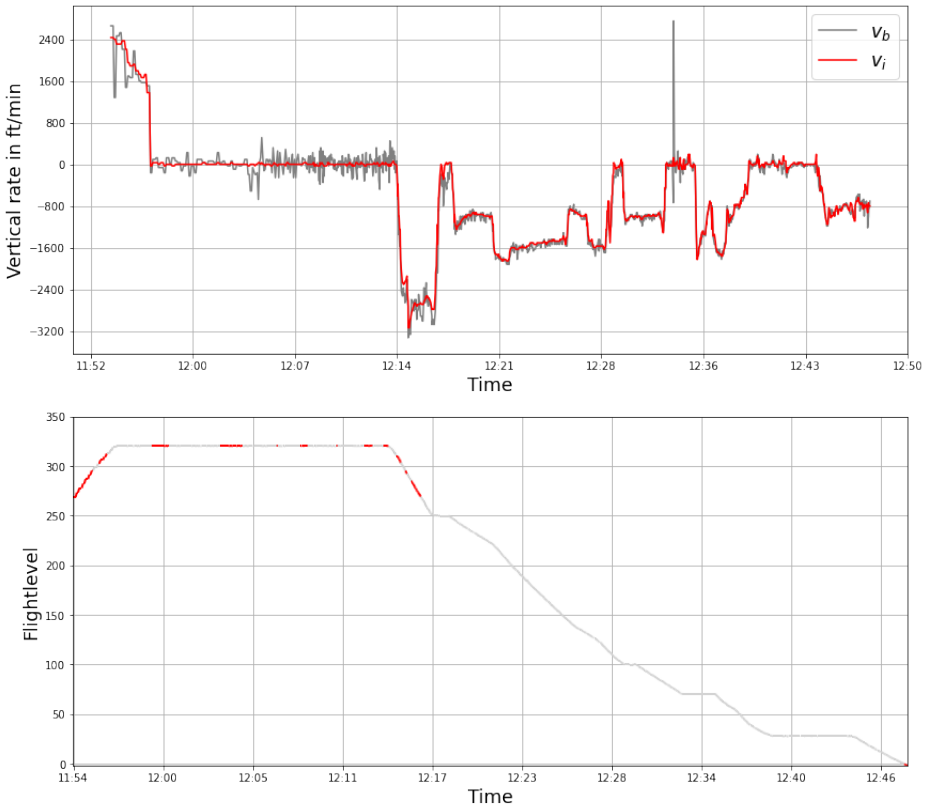

Figure 4.10: An example where extra radar data is included. Top: barometric vertical rate shows extra peak around 12:34 UTC. Bottom: result of the algorithm plotted on flight level over time.

4.1.2 Measure turbulence severity

In the analysis of wake turbulence encounters, it would be helpful if it were possible to measure the intensity of turbulence. When validating the algorithm for en-route air traffic we used, as Olive and Sun [10] did in their research, heatmaps to give a clear overview of the areas where turbulence was detected. The colors in the heatmap were based on the average of thresholds of the flights crossing a grid cell and should give insight in the severeness of turbulence in that grid cell.

As mentioned before, we question whether the threshold is a good measure for the severeness of turbulence. It might be useful for comparing the average level of turbulence experienced by aircraft in the entire flight to other aircraft but since it is a constant and turbulence intensity differs during the flight, it will not be able to distinguish different intensities. The value of $\Delta\sigma$ might give a better indication for this.

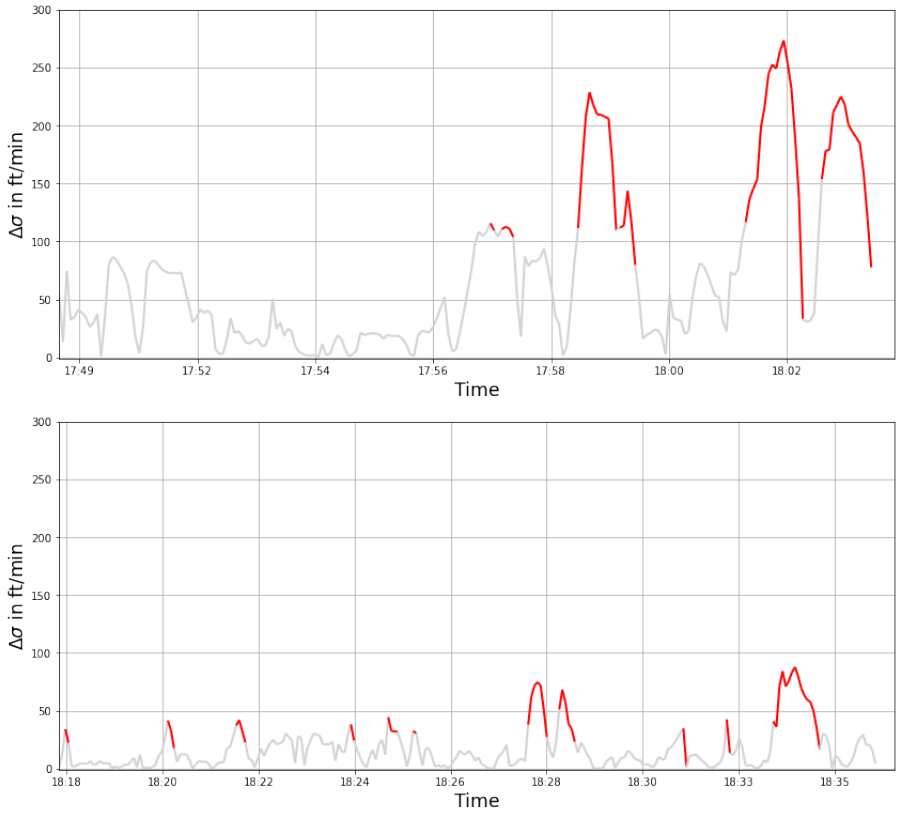

Figure 4.11: Difference in standard deviation $\Delta\sigma$ of two flights in similar circumstances, with detected turbulence in red.

We compare two medium aircraft flying the same route from London Heathrow Airport to Amsterdam Airport Schiphol half an hour apart, landing in equal weather circumstances. In Figure 4.11, $\Delta\sigma$ is plotted over time for two aircraft with the values above threshold in red. While we expected to see similar values for both aircraft due to the constant circumstances, we observe a completely different pattern in the two figures. The top figure shows the result of an aircraft of type B737 with a threshold of 110.5. The bottom figure shows the result of an aircraft of type A320 with a threshold of only 31.8. This big difference might of course be an exception, for example due to the heavy wind on that day. Therefore, we compare thresholds of all flights from London Heathrow Airport to Amsterdam Airport Schiphol on a day with little wind and we find thresholds varying from 30 to 75. What is a striking observation is that aircraft of type B737 have thresholds between 65 and 75, whereas the other types have values between 30 en 40. This suggests that noise varies over aircraft type and besides the threshold also $\Delta\sigma$ might not be a good measure for the severeness of turbulence.

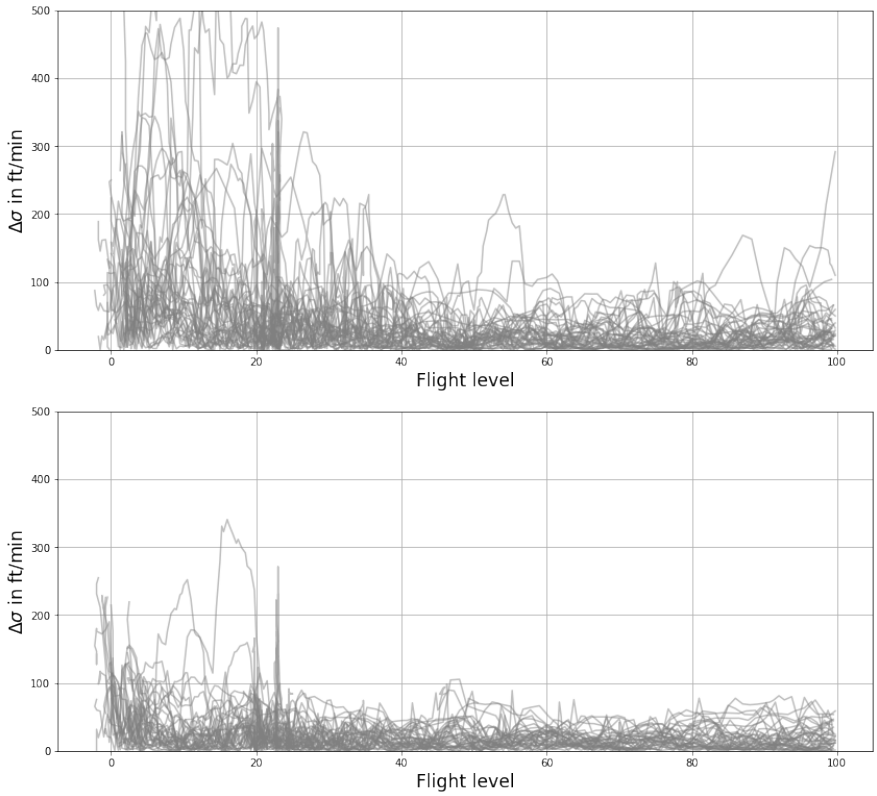

Figure 4.12: Difference in standard deviation of final 100 flight levels of aircraft of type B737 (top) and A320 (bottom).

In Figure 4.12, we plotted $\Delta\sigma$ for flights entering the TMA at SUGOL in the week from 27-10-2020 to 02-11-2020. Since all aircraft fly the approximate same route in the TMA, we will compare the final 100 flight levels of all flights. The top figure shows the result for aircraft of type B737. The bottom figure shows the result for aircraft of type A320. We observe higher and more deviating values for aircraft of type B737, but also aircraft of type A320 have some deviating values. For other types of aircraft, similar results are obtained. Although the results for aircraft of type B737 seem higher on average, we do not observe a clear trend. We conclude that there is not an overall trend per aircraft type, but that diverging values exist for all types.

To be able to compare results of all aircraft, we want to convert the data into a uniform scale. Normalisation, or min-max scaling, scales the data to an interval between zero and one. The maximum value gets normalised value one and the minimum value gets normalised value zero [6]. We go back to the example of the two aircraft flying from London Heathrow Airport to Amsterdam Airport Schiphol half an hour apart and apply normalisation to $\Delta\sigma$. The non-normalised results for $\Delta\sigma$ were already shown in Figure 4.11, the normalised results are shown in Figure 4.13. These figures look promising, since both aircraft show similar values now. However, if the maximum value of $\Delta\sigma$ is one for each flight, it is still impossible to compare turbulent strength. Since for one aircraft experiencing some weak turbulence only, this weak turbulence peak is scaled to have a top at one, but for another aircraft experiencing severe turbulence, this severe turbulence peak is scaled to have a top at one, as well. What we need is a scaling to have the non-turbulent values approximately in the same range, but outliers to be more visible and not in a bounded range.

We propose to apply standardisation. Standardisation scales the data to have mean zero and standard deviation one. The formula for standardisation is

$$\Delta\sigma'_j = \frac{\Delta\sigma_j - \overline{\Delta\sigma}}{\sigma(\Delta\sigma)}, \tag{4.1}$$

where $\overline{\Delta\sigma}$ and $\sigma(\Delta\sigma)$ are the mean and standard deviation of all $\Delta\sigma_j$, respectively. We use the same two flights as before to demonstrate standardisation. The standardised results are shown in Figure 4.14. An advantage of standardisation is that values are not scaled to a bounded range thus outliers are not so much affected [6]. We observe that most values lie between minus one and one with some peaks varying in size. For this example, the two figures were expected to have similar values since the aircraft flew in similar circumstances. To check if deviations vary for other turbulent flights, we look at a larger scale. In Figure 4.15, we standardised the results from Figure 4.12. We observe the values to be more on the same scale than before the standardisation.

Due to the computation of the threshold, every flight has a threshold of 1.2. This means that the threshold cannot be used for comparing the average level of turbulence

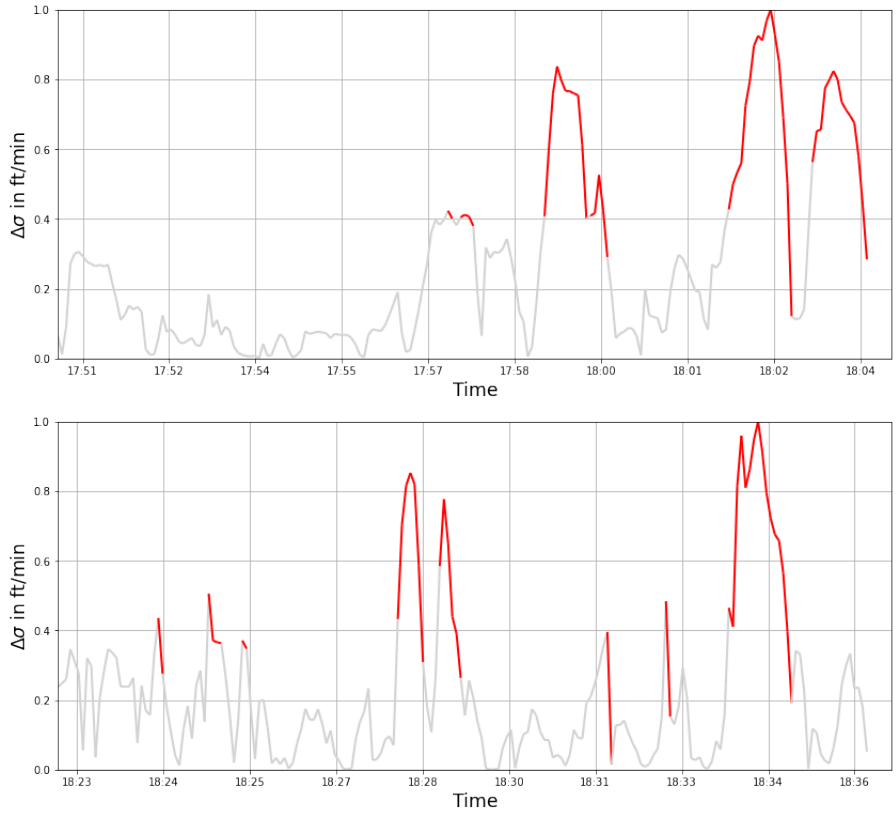

Figure 4.13: Normalised difference in standard deviation of two flights in similar circumstances, with detected turbulence in red.

experienced by aircraft anymore. Since we are interested in specific turbulence cases, this is not a problem for this research. The advantage of this is that $\Delta\sigma'$ seems more useful for comparing turbulence in specific cases.

To check whether $\Delta\sigma'$ can be used as a measure for the strength of turbulence we use the reported wake turbulence situations, of which we know whether it was experienced as weak, moderate or severe turbulence. In Figure 4.16, $\Delta\sigma'$ is plotted for a flight where severe turbulence was reported. We clearly see a high peak in the plot at 00:33 UTC, suggesting that $\Delta\sigma'$ is high for severe turbulence. However, comparing the results of reported moderate to weak wake turbulence shows less significant results. The top two figures in Figure 4.17 show the results for flights with moderate wake turbulence reported around 8:32 UTC and 10:12 UTC, respectively. The bottom figure shows the result for a flight with weak turbulence reported around 9:25 UTC. According to the values of $\Delta\sigma'$, the aircraft in the first figure seems to have experienced weaker turbulence than the aircraft in the other two figures. As

the intensities as stated in the data are mainly based on pilot reports and one pilot can describe turbulence as weak while the other describes it as moderate, this could be an explanation for the obtained results. Research on a larger scale is needed to determine whether $\Delta\sigma'$ is a good measure for the strength of turbulence.

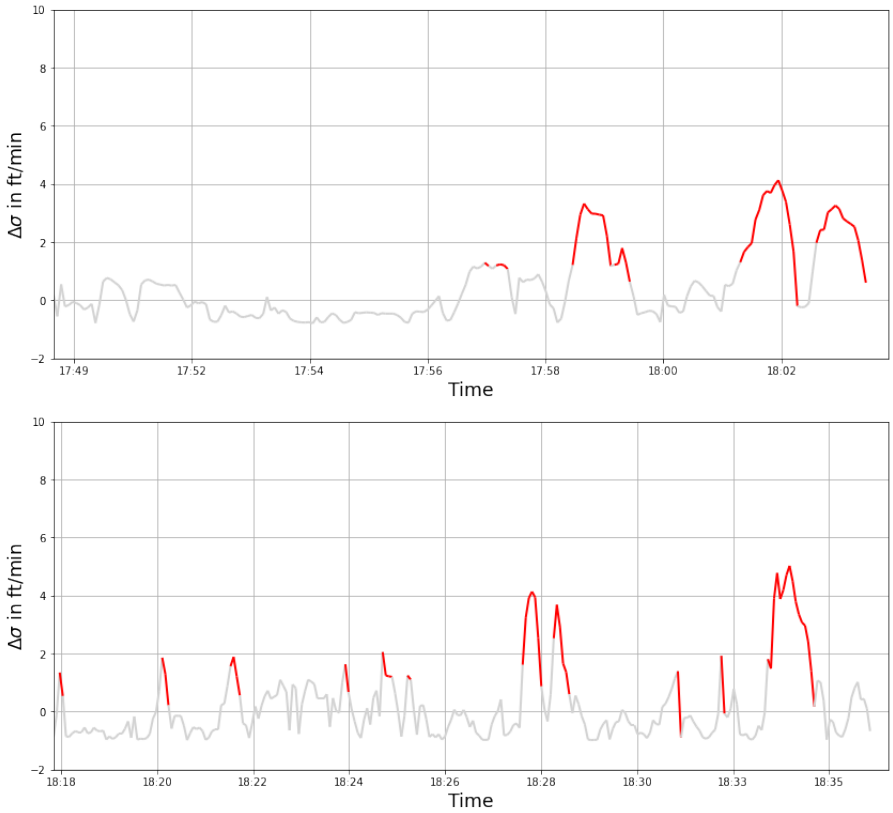

Figure 4.14: Standardised difference in standard deviation $\Delta\sigma'$ of two flights in similar circumstances, with detected turbulence in red.

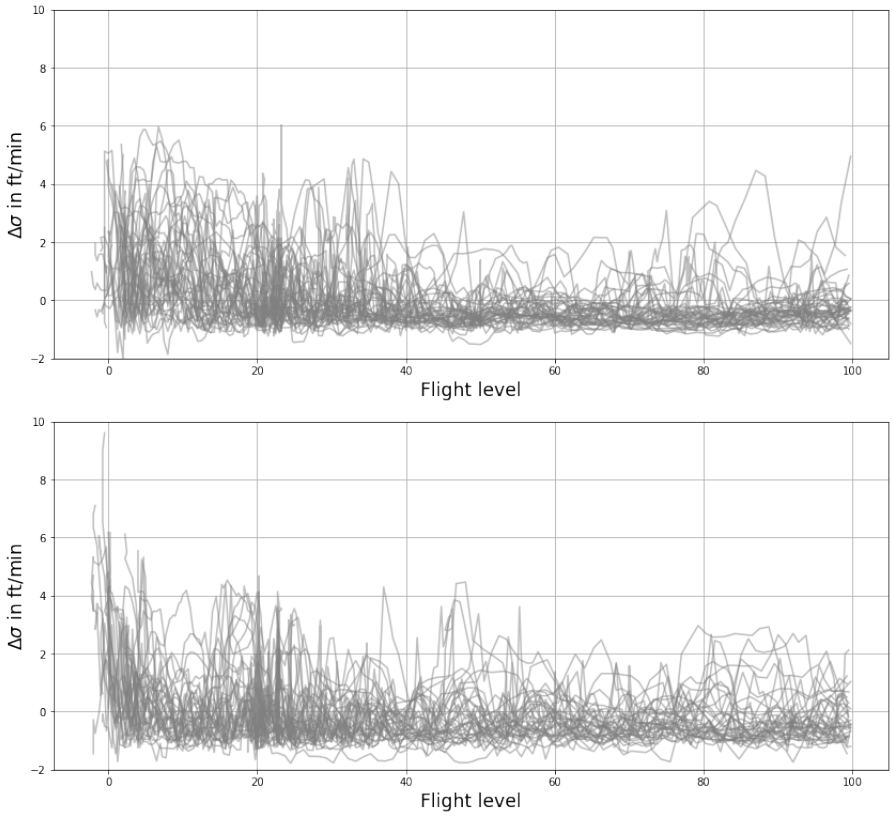

Figure 4.15: Standardised difference in standard deviation $\Delta\sigma'$ of final 100 flight levels of aircraft of type B737 (top) and A320 (bottom).

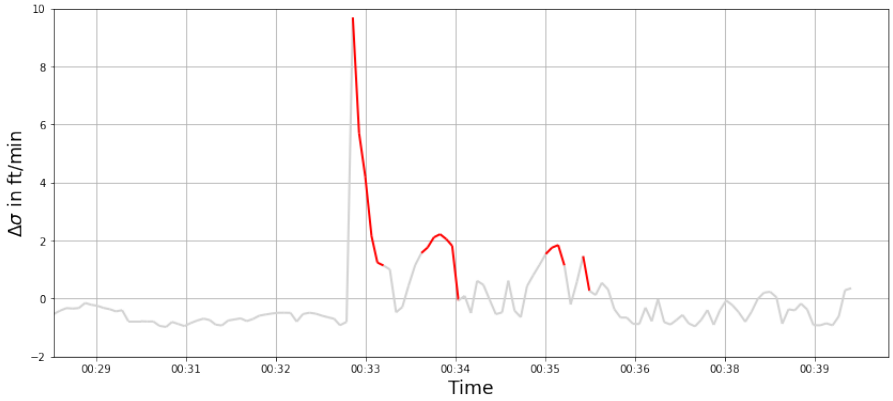

Figure 4.16: Standardised difference in standard deviation $\Delta\sigma'$ of a flight where severe wake turbulence is reported.

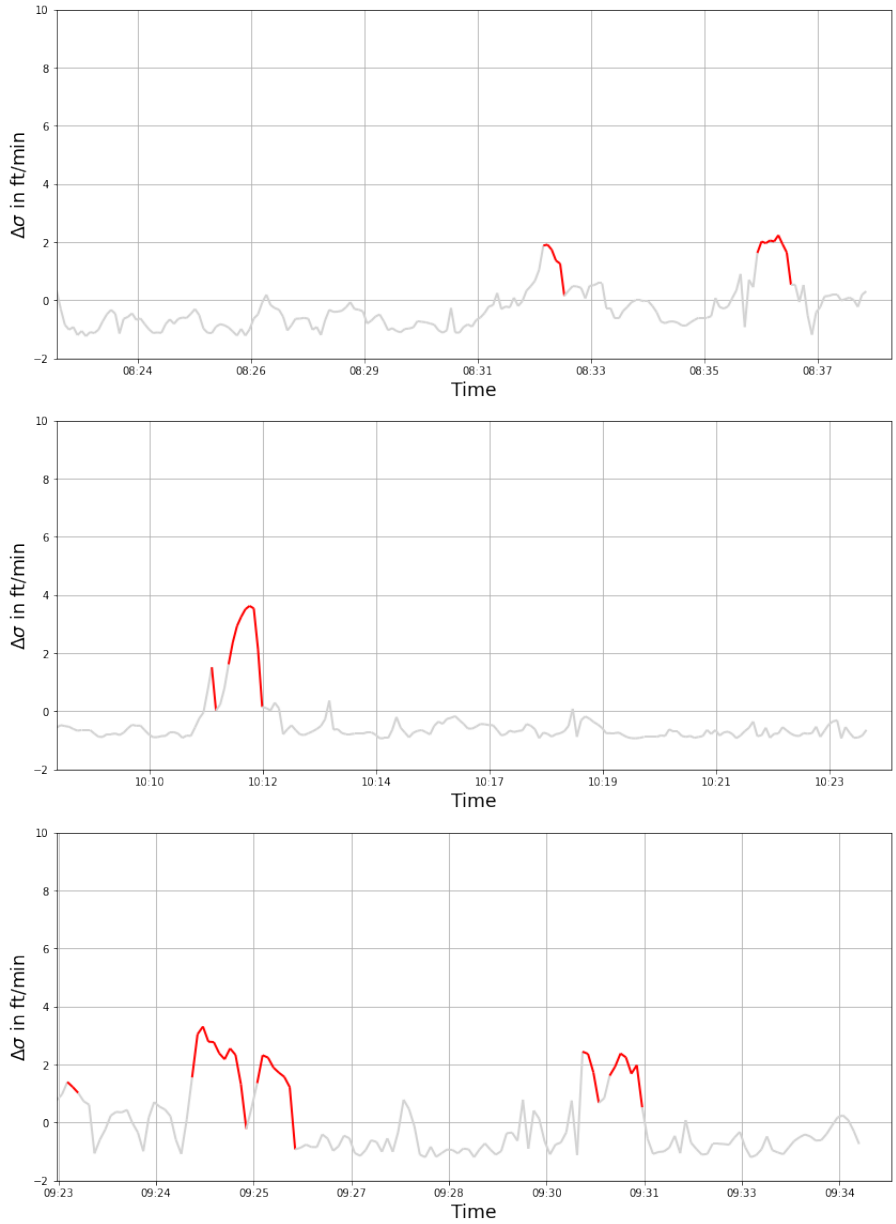

Figure 4.17: Standardised difference in standard deviation $\Delta\sigma'$ of flights where moderate (top and middle) and weak (bottom) wake turbulence is reported.

4.2 Distinguish wake turbulence

So far, we have analysed known wake turbulence encounters and concluded that the algorithm can detect most of the available cases. However, only a few incidents are reported by pilots and more wake turbulence encounters happen, mostly in final approach. One of the goals of the thesis is to get insight in the number of wake turbulence encounters and therefore we want to be able to distinguish wake turbulence from the other detected turbulence.

When validating the algorithm for approaching air traffic, we have seen that turbulence caused by weather effects is detected by the algorithm. Therefore, we will focus on situations where these factors are minimized. For example the situation sketched in Figure 4.18. There were no clouds and a windspeed of only three knots according to the METAR of Amsterdam Airport Schiphol. But we still observe some turbulence to be detected in final approach, possibly caused by wake vortices. What stands out is that three aircraft, entering the TMA at SUGOL, fly over their own future position, from West to East, making a turn to the South and flying final approach to the North, where they will experience turbulence. Since wake vortices go down, it might be the case that the detected turbulence is turbulence caused by their own wake vortices. Analysis on a larger scale, in the same circumstances, is needed to draw conclusions.

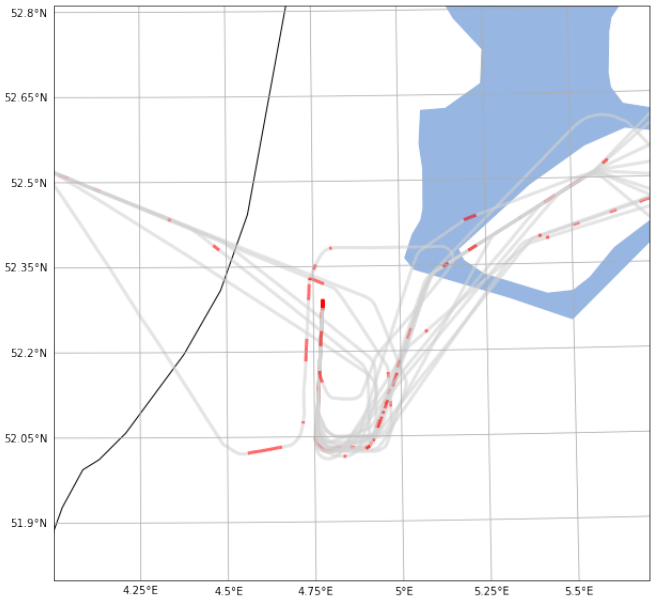

Figure 4.18: Approaching air traffic in a time period with little winds and no clouds, possible wake turbulence is detected in final approach.

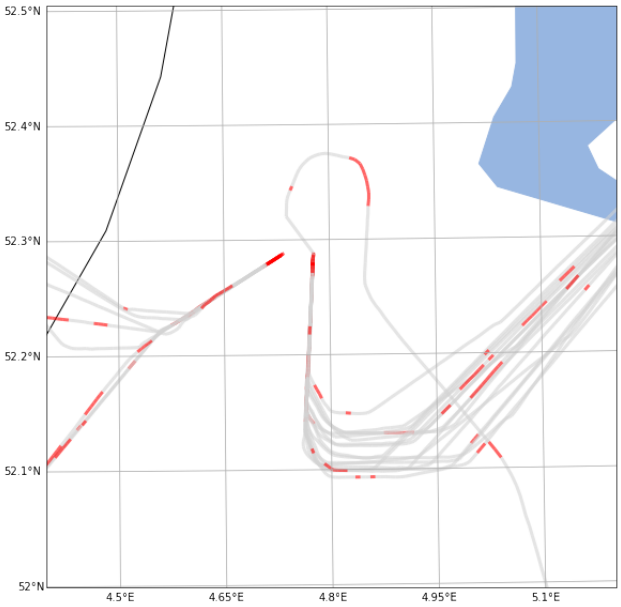

Figure 4.19: Approaching air traffic in a time period with little winds and no clouds, possible wake turbulence is detected in final approach.

We analyse a second situation with windspeeds of only two knots, with no rain and no clouds reported. Aircraft approaching in a time period of 30 minutes are shown in Figure 4.19. Despite the non turbulent weather circumstances, still some turbulence is detected during the final approach. Both in this example and in the previous example, the ICAO separation minima are met. This does not exclude the possibility for the detected turbulence to be wake turbulence. Besides it being caused by wake turbulence, it is also possible that a sudden decrease in speed caused by extending the landing gear or using wing flaps led to turbulence. However, we did not observe this in any analysed situation.

To confirm detected turbulence to be wake turbulence one might analyse other sources of data. For example, the distance to the aircraft in front and types of both leading and following aircraft can give insight in whether a wake vortex could have been strong enough to cause wake turbulence. Moreover, wake turbulence is sometimes visible in the roll angle, since a wake can have a rolling effect on an aircraft. An example where the roll angle shows extreme values during a reported wake turbulence encounter is shown in Figure 4.20. Wake turbulence is reported by a pilot around flight level 70. This reported turbulence is detected by the algorithm as shown in the top figure. At the time of the turbulence encounter, the plot of the roll angle in the bottom shows an extreme peak.

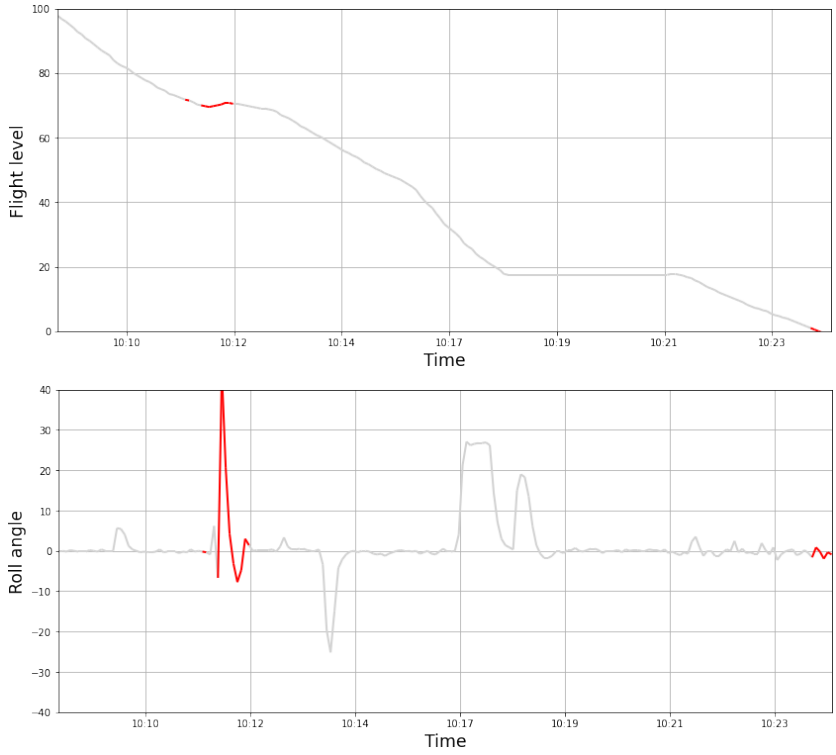

Figure 4.20: Pilot-reported wake turbulence encounter around flight level 70 detected by the algorithm. Result plotted on flight level in the top and on roll angle in the bottom.

We conclude that with favorable weather circumstances it is likely that wake turbulence is detected. However, in heavy weather it is hard to distinguish wake turbulence from turbulence caused by the weather. Turbulence caused by wind and turbulence caused by wake vortices can both result in a sudden drop in altitude and/or shaking of the aircraft. Not only for the algorithm and analysis of the results, but also for pilots themselves is it sometimes hard to distinguish different causes of turbulence.

For example, much wake turbulence and windshear is communicated to air traffic controllers at Amsterdam Airport Schiphol where wind flowing over the Amsterdam Forrest causes mechanical turbulence to approaching aircraft. An example where this could be the case is shown in Figure 4.21. A Southwestern wind with speeds between 15 and 20 knots is reported. Turbulence is detected for many aircraft in the final part before landing. However, we have already seen that wind causes much turbulence, also for aircraft not flying over the Amsterdam Forrest. So we cannot conclude that this detected turbulence is actually the mechanical turbulence caused by the Amsterdam Forrest, yet another example where explaining turbulence is difficult.

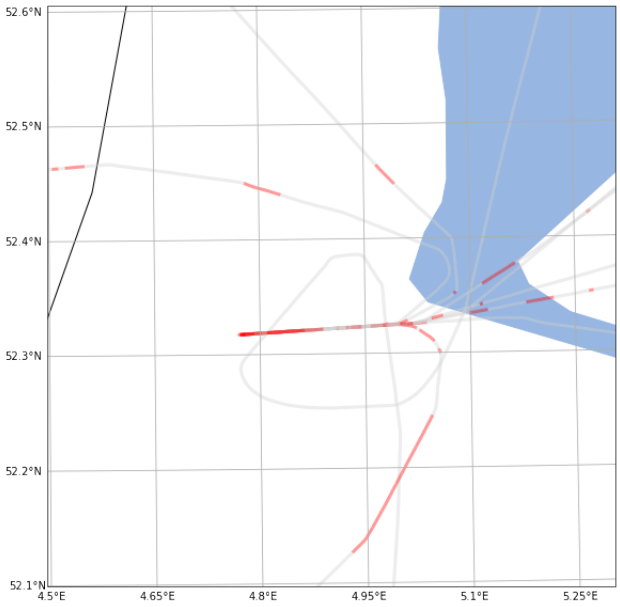

Figure 4.21: Possible mechanical turbulence caused by wind flowing over the Amsterdam Forrest visible right before landing.

Chapter 5

Conclusions and discussion

The goal of this thesis was to investigate whether the algorithm for detecting and measuring turbulence proposed by Olive and Sun [10] can be used for approaching air traffic, as well, and to analyse the applicability for analysing wake turbulence encounters. The conclusions and suggestions for future work are discussed in this chapter.

5.1 Conclusions

We started with the validation of the algorithm. Where Olive and Sun implemented and analysed the algorithm for en-route air traffic only, we extended the analysis to approaching air traffic with a focus on wake turbulence. Therefore, besides examining a consistency of turbulence across aircraft and over time for en-route air traffic we validated the algorithm for approaching air traffic by also looking at a consistency with reported heavy weather circumstances and reported wake turbulence encounters. We concluded that the algorithm was able to detect 43.8% reported wake turbulence encounters.

To improve the detection of turbulence by the algorithm we proposed to implement a moving standard deviation instead of using the standard deviation of a small number of time windows only. Although many smaller periods of turbulence are detected, making the results more unclear, we still concluded this adaptation to be an improvement to the algorithm since this made it possible to detect in total 68.8% of the reported wake turbulence encounters.

Furthermore, we experimented with the data by reducing the data set to descent data only. We did detect a reported wake turbulence encounter we did not detect before using descent data only. However, by doing this the assumption made by Olive and Sun, that this algorithm and threshold works well because an aircraft will always

experience turbulence during a flight and this turbulence will never last the entire flight, is ignored. Therefore, we concluded that this is not an improvement for large scale analysis.

For a more precise detection of turbulence we included extra raw radar data. This did not result in extra detection for the known pilot-reported wake turbulence encounters, due to the fact that peaks in barometric vertical rate were filtered out as outlier. We analysed the possibility to exclude the filtering, but concluded that this would not help for the analysis of wake turbulence encounters due to an increase in false positives.

To analyse wake turbulence encounters, it is helpful to be able to measure the severity of the turbulence detected. We concluded that the computed threshold and difference in standard deviation are not able to give a good indication of severity of turbulence and proposed to standardise the difference in standard deviation and use this as a measure for the severity. We saw the standardised values of the difference in standard deviation to be more comparable and the analysis of a severe reported wake turbulence encounter suggested that this might indeed be a good measure for the level of turbulence.

Finally, we looked into the possibility to distinguish wake turbulence from other detected turbulence to be able to get insight in the number of wake turbulence encounters. We concluded that with favorable weather circumstances it is likely that turbulence detected in final approach is caused by wake vortices. However, with heavy wind and rain too much turbulence is detected to be able to distinguish between turbulence caused by the weather and turbulence caused by wake vortices. Also, heavy wind causes wake vortices to dissipate more quickly which makes it less likely that wake turbulence is experienced.

All together, we conclude that the algorithm can be used to detect turbulence for approaching air traffic. However, it is hard to distinguish wake turbulence if effects of heavy weather cannot be ruled out. To measure the intensity of turbulence, standardising is proposed. But, this needs extra analysis on larger scale to draw conclusions for the applicability.

5.2 Discussion and future work

The assumption made by Olive and Sun on which the turbulence detection is based is that an aircraft will always experience turbulence during a flight and this turbulence will never last the entire flight. For this research, data collected by radars in the Netherlands is used covering an area of approximately 200 kilometers around the country. This means that for analysis of flights approaching Amsterdam Airport Schiphol departing outside this area, we do not take the entire flight into account.

Although we have seen good results, further research on this topic may use data of the entire flight, if available, to obtain even more precise results.

Besides extending the radar data to other parts of the world, more data on reported wake turbulence would also be helpful for further analysis. So far, standardising the difference in standard deviation looks promising for determining the intensity of turbulence. We saw, for example, a severe wake turbulence case that showed an extreme value suggesting that higher values of the new measure indicate more severe turbulence. However, a clear trend for weak and moderate reports was not visible. Future work might include to analyse more wake vortex reports to see if a trend exists and thus if the standardised difference in standard deviation is a good measure for severity of turbulence.

As one of the ideas is to use this algorithm to create a warning system for air traffic controllers, it is possible to research the prediction of wake turbulence using machine learning algorithms. Much data is available, for example on wind and aircraft speed, that is correlated to the strength of the wake vortex and the effect of it on the trailing aircraft. If more wake vortex reports become available, machine learning algorithms can be trained and tested on larger data sets leading to better algorithms.

Another application of this algorithm might be to get insight in the number of wake turbulence encounters which can be helpful in the analysis of RECAT-TBS once it is implemented and in use. We have concluded that the algorithm can be used for detecting wake turbulence in situations where weather effects are ruled out. This means that for those situations it is possible to get insight in the number of wake turbulence encounters and is it possible to compare results. This will specifically be useful when analysing wake turbulence after implementation of RECAT-EU. For the effect after implementation of TBS it will be less useful, since TBS will decrease separation between aircraft mostly in strong headwind, where a wake vortex dissipates more quickly. More research on distinguishing wake turbulence can be done, possibly in combination with wake turbulence prediction algorithms, to also be useful in heavier weather circumstances.

Bibliography

[1] G.B. van Baren. *Benefits analysis of RECAT-EU for Schiphol Airport*. NLR, Aug. 2016.

[2] EUROCONTROL. *ASTERIX Part 1 (SPEC-149)*. 3rd ed. Dec. 2020. ISBN: 978-2-87497-028-3.

[3] EUROCONTROL. *Five-Year Forecast 2020-2024*. Nov. 2020.

[4] EUROCONTROL. *System Track Data*. 19th ed. Dec. 2020. ISBN: 978-2-87497-028-3.

[5] EUROCONTROL. *Time Based Separation (TBS)*. URL: http://recat-project.eu/time-based-separation-tbs. (accessed: 09.03.2021).

[6] J. Han, M. Kamber, and J. Pei. In: *Data Mining: Concepts and Techniques*. 3rd Edition. Boston, 2012, pp. 103–110. ISBN: 978-0-12-381479-1. DOI: https://doi.org/10.1016/B978-0-12-381479-1.00003-4.

[7] Ministère de la transition écologique et solidaire. *A fine-tuned wake vortex recategorisation*. URL: https://www.ecologie.gouv.fr/sites/default/files/RECAT_EU.pdf. (accessed: 09.03.2021).

[8] NATS. *NATS: Intelligent Approach*. URL: https://www.nats.aero/features/intelligent-approach/. (accessed: 20.02.2021).

[9] NBBA. *Mode S Transponders*. URL: https://nbaa.org/aircraft-operations/communications-navigation-surveillance-cns/mode-s-transponders/. (accessed: 10.03.2021).

[10] X. Olive and J. Sun. "Detecting and Measuring Turbulence from Mode S Surveillance Downlink Data". In: *ICRAT 2020*. Aug. 2020.

[11] Schiphol. *Traffic review 2020*. 2020. URL: https://www.annualreportschiphol.com/trafficreview2020. (accessed: 18.04.2021).

[12] SKYbrary. *Inertial Reference System (IRS)*. URL: https://www.skybrary.aero/index.php/Inertial_Reference_System_(IRS). (accessed: 20.03.2021).

[13] SKYbrary. *RECAT - Wake Turbulence Re-Categorisation*. URL: https://www.skybrary.aero/index.php/RECAT_-_Wake_Turbulence_Re-categorisation#Re-categorisation. (accessed: 10.03.2021).

[14] SKYbrary. *Separation Standards*. URL: https://www.skybrary.aero/index.php/Separation_Standards. (accessed: 10.03.2021).

[15] SKYbrary. *Wake Vortex Propagation and Decay*. URL: https://www.skybrary.aero/index.php/Wake_Vortex_Propagation_and_Decay. (accessed: 20.02.2021).

[16] SKYbrary. *Wake Vortex Turbulence*. URL: https://www.skybrary.aero/index.php/Wake_Vortex_Turbulence. (accessed: 20.02.2021).

[17] J. Sun. *The 1090 Megahertz Riddle: A Guide to Decoding Mode S and ADS-B Signals*. 2nd ed. TU Delft OPEN Publishing, 2020.

Appendix A

List of Symbols

v_b	barometric vertical rate
v_i	inertial vertical velocity
$\sigma_{v_{b,j}}$	standard deviation of barometric vertical rate in time segment j
$\sigma_{v_{i,j}}$	standard deviation of inertial vertical velocity in time segment j
$\Delta\sigma_j$	absolute difference between $\sigma_{v_{b,j}}$ and $\sigma_{v_{i,j}}$
$\Delta\sigma$	column with $\Delta\sigma_j$ for all j

Appendix B

List of Abbreviations

ACAS	Airborne Collision Avoidance System
ASTERIX	All purpose Structured EUROCONTROL Surveillance Information Exchange
BDS	Comm-B Data Selector
EHS	Enhanced Surveillance
ELS	Elementary Surveillance
EUROCONTROL	European Organistion for the Safety of Air Navigation
FAF	Final Approach Fix
FL	Flight Level
IAF	Initial Approach Fix
IF	Intermediate Approach Fix
ICAO	International Civil Aviation Organisation
KNMI	Royal Netherlands Meteorological Institute
LVNL	Air Traffic Control the Netherlands
MRS	Minimum radar separation
METAR	Meteorological Aerodrome Report
MHR	Meteorological Hazard Report
MRAR	Meteorological Routine Air Report
NATS	National Air Traffic Services of the UK
NM	Nautical Mile
RECAT-EU	Wake Vortex Re-Categorisation
RECAT-TBS	Wake Vortex Re-Categorisation and Time Based Separation
TBS	Time Based Separation
TMA	Terminal Manoeuvring Area
WTC	Wake Turbulence Category

Appendix C

Glossary

Approaching air traffic	Air traffic descending to land.
ARTAS	System that processes surveillance data.
ARTIP	IAF above Flevoland.
Barometric vertical rate	Measure of vertical rate obtained from barometer measurements.
Cruise	Phase of the flight after climb and before descent.
En-route air traffic	Air traffic outside TMAs containing final part of climb, cruise and begin of descent.
Final approach	Final segment of descent where aircraft is lined up with the runway for landing.
Final approach fix	A specified point where final approach starts.
Flight level	Aircraft's altitude above sea-level in hundreds of feet.
Go around	An aborted landing.
Ground speed	Aircraft's speed with respect to the ground.
Magnetic heading	Angle between the heading of the aircraft and magnetic North.
METAR	A weather report formulated at an airport every half an hour.
Mode S radar	A secondary surveillance radar technique.
Inertial vertical velocity	Measure of vertical rate obtained from fusing barometer altitude and inertial acceleration.
Initial approach	Segment of descent from IAF to IF or FAF.
Initial approach fix	A specified point where initial approach starts.
Intermediate approach	Segment of descent from IF to FAF, not always included in approach procedure.
Intermediate approach fix	A specified point where intermediate approach starts.
Roll angle	Rotation of the aircraft around the longitudinal axis.
RIVER	IAF above Rotterdam.
SUGOL	IAF above the North Sea.
True airspeed	Aircraft's speed with respect to the air.
Track angle	Angle between track and true North.
Wake vortex	Turbulent airflow that follows an aircraft.